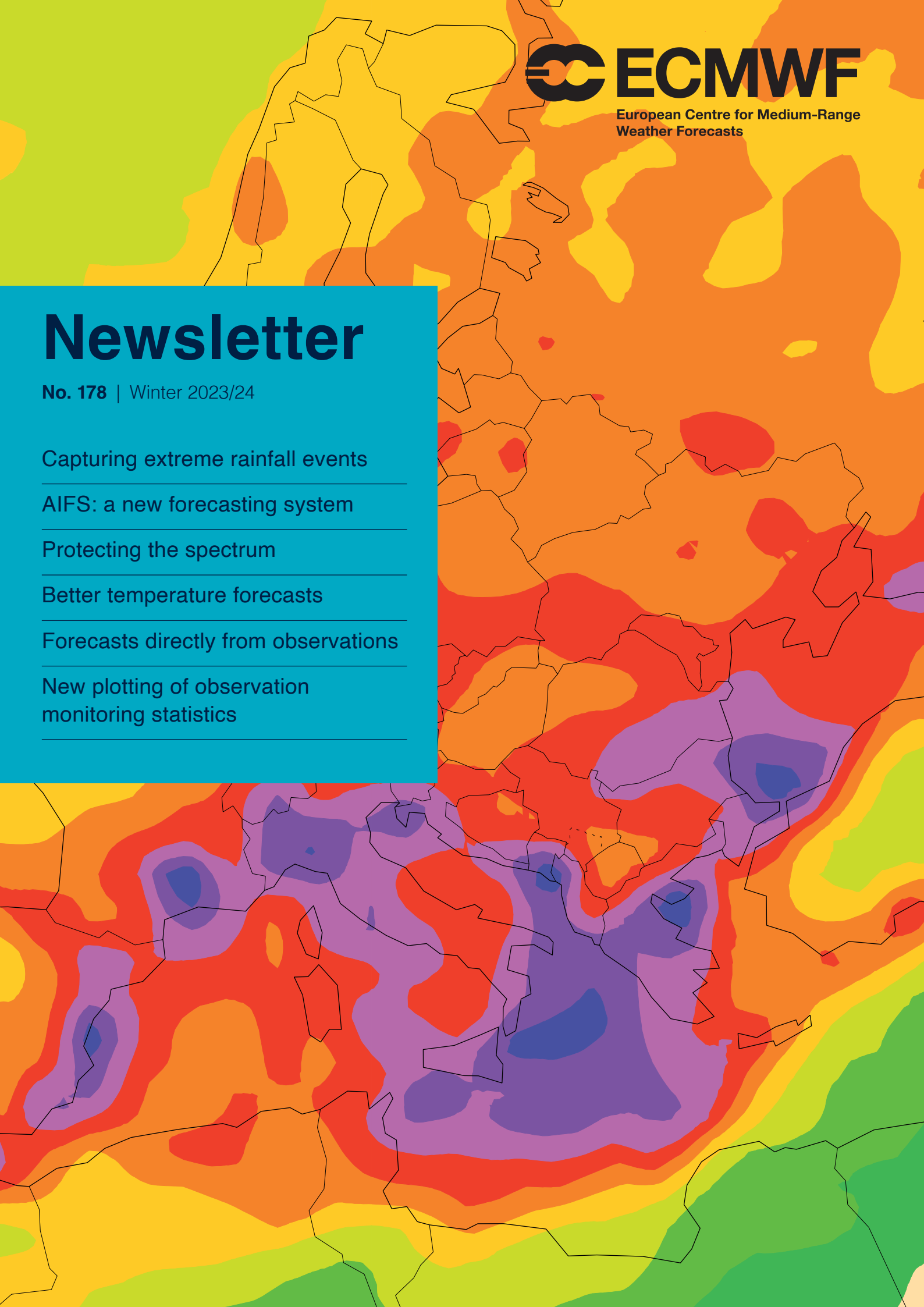

ECMWF

European Centre for Medium-Range Weather Forecasts

Newsletter

No. 178 | Winter 2023/24

Publication policy

The ECMWF Newsletter is published quarterly. Its purpose is to make users of ECMWF products, collaborators with ECMWF and the wider meteorological community aware of new developments at ECMWF and the use that can be made of ECMWF products. Most articles are prepared by staff at ECMWF, but articles are also welcome from people working elsewhere, especially those from Member States and Co-operating States.

The ECMWF Newsletter is not peer-reviewed.

Any queries about the content or distribution of the ECMWF Newsletter should be sent to Georg.Lentze@ecmwf.int

Guidance about submitting an article and the option to subscribe to email alerts for new Newsletters are available at *www.ecmwf.int/en/about/media-centre/media-resources*

The pace is quickening

Only a few months have passed since I told you about the alpha version of our Artificial Intelligence/Integrated Forecasting System (AIFS), and it is time to update you on our latest advances in machine learning. The first development is that we have published a new alpha version of the AIFS, which particularly increases performance for weather parameters at the Earth's surface. The new version decreases the horizontal grid spacing from 111 km to 28 km, it increases the number of predicted fields, and it uses a new model structure combining graph neural networks with transformers. This is clearly not the final word, but we are very pleased with the results achieved so far. An introduction to the AIFS is included in this Newsletter, but for more up-to-date information I refer you to the AIFS blog on the ECMWF website.

At the same time, we are working on an even more radical idea: using machine learning to make weather forecasts directly from meteorological observations. The AIFS and other machine learning prediction systems rely on reanalysis datasets such as ECMWF's ERA5 for training, and on initial conditions through data assimilation. We are now exploring if a forecasting system based on machine learning can be trained and initialised directly from meteorological observations. First steps in that direction are outlined in this Newsletter. A joint project with ECMWF Member States will also explore machine-learning-assisted forecasting methods, from global to local scales.

Meanwhile, the development of our classical forecasting system continues. Later this year, our Integrated Forecasting System (IFS) is due to be upgraded to Cycle 49r1. This will, for example, include changes that improve forecasts of two-metre temperature. Related changes are made both to the physics of the forecasting system and to data assimilation, including the assimilation of temperatures from SYNOP observations to arrive at the best possible initial conditions. Other topics covered include an introduction to a new on-demand system to visualise statistics on the quality and availability of different components of the observing system used by ECMWF. There is also a 'Viewpoint' article on a new European group formed to articulate concerns over Radio Frequency Interference at World Radiocommunication Conference (WRC) meetings. This is important as it concerns the integrity of the global observing system for weather and climate.

Another article looks at the quality of our forecasts of extreme rainfall events, and there is an update on the development of the global component of the Weather-Induced Extremes Digital Twin. This is being created at ECMWF as part of the European Commission's Destination Earth initiative. The digital twins will also benefit from progress in machine learning, so it is not just our standard weather forecasts that will be able to make use of this field of study.

Florence Rabier
Director-General

Contents

Editor Georg Lentze • **Typesetting & Graphics** Anabel Bowen • **Cover** Version of first figure on page 3

doi: 10.21957/1a8466ec2f

Capturing extreme rainfall events

Tim Hewson

Society is naturally interested in extreme rainfall events and whether they can be predicted. This item looks at 14 such events from summertime 2023, from various model-output-related perspectives.

The scatterplot references 14 extreme rainfall events between June and September 2023, with red markers showing 24-hour totals from single rain gauges, selected to try to represent 'peak rainfall' for each event. The main basis for selection was media reports of flooding events, which varied in severity. Whilst manual quality control of gauge data has been applied, errors probably still exist. These concern, for example, the measurement start/end times, which can sometimes be hard to disentangle. Probably for all events, the true peak rainfall was also higher than shown, due to imperfect data coverage. For example, whilst the Madeira value should be representative, due to very high gauge density, the Libya total is probably a large underestimate, due to lack of observations.

ECMWF's performance

The first question we then pose is: was ECMWF's Integrated Forecasting System (IFS), in ensemble form, able to foresee these events? To answer, we show with blue markers the maximum forecast 24 h rainfall value for the nearest IFS grid point, using a lighter shade for a 4-day lead, and darker for a 2-day lead. In each case, 52 medium-range runs from the same start time are referenced, for 3x24 h periods of validity that start at 12 UTC the day before the valid date, and 00 and 12 UTC on that date. In this way, we allow for uncertainty in rainfall report timing, and/or accommodate IFS forecast timing errors. These can thus be considered wet outlier forecasts for the said events. For a set of forecast runs to be quantitatively useful, in advising a forecaster what rainfall amounts to allow for in any warnings, values need to be greater than what was observed, so that the eventual outcome lies within the ensemble range. This criterion is met for only two cases – the Toledo and Beijing events. Meanwhile one can also see, somewhat surprisingly, that day 2 forecasts are no better overall, by this metric, than day 4. One possible interpretation is that synoptic patterns are already well captured at day 4, and that ensemble perturbations, perhaps mainly those that arise from the stochastic physics, are then causing just semi-random oscillations in the most extreme rainfall within the ensemble.

Of course, it has long been recognised that gridbox rainfall values from a model cannot represent localised extremes at point scale, because of factors such as sub-grid variability and biases, both of which depend on the situation (geographical and meteorological). The finer the resolution of the model, the smaller any shortfall should be. So what resolution is required to capture point-relevant variability? The European map plot shows the top value in 15,000 realisations from 20 years of operational re-forecasts, at 9 km

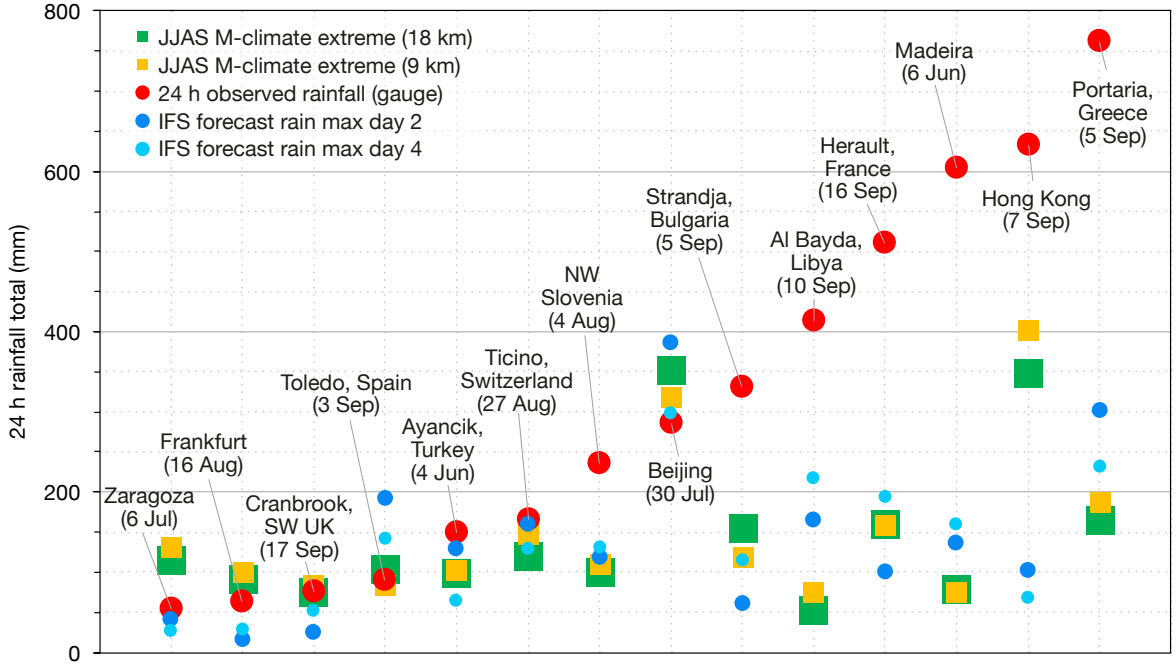

Some newsworthy extreme rainfall events from June – September 2023. Observed 24 h rainfall peaks (mm) are shown in red, in ranked order, with labels showing location and the main date (UTC). Maximum rainfall values forecast for these sites, in 00 UTC medium-range forecasts in the Integrated Forecasting System (IFS), from four and two days before the given date, are shown in light and dark blue respectively. Maximum rainfall realised in about 15,000 re-forecasts for the same four months, from scans of lead times of 1, 2,.. 7 days, are also shown, for the same sites, in green for IFS Cycle 47r3 (18 km resolution, 2002–2021) and yellow for Cycle 48r1 (9 km resolution, 2003–2022).

resolution (IFS Cycle 48r1), indicating a propensity for higher extremes in southern Europe. On the scatterplot, we show with squares, for the designated locations, these model-climate extremes as reference points for the depicted forecasts, for 9 km (yellow) and 18 km (green, Cycle 47r3) resolutions. Whilst 9 km resolution delivers marginally higher extremes than 18 km, overall the difference is smaller than one might expect. The reason is probably model physics changes in 48r1, which reduced rainfall in some net sense to address a known, global, over-prediction bias. Where forecast values lie above these thresholds, it can act as an alert that something very extreme may happen (without indicating likely values). This behaviour can be seen for about five of the 14 cases, which include three of the wettest five events. Indeed, this type of comparison strategy underpins the EFI (Extreme Forecast Index) and SOT (Shift Of Tails) metrics, which are widely used to anticipate extreme weather. So, whilst there is a huge shortfall in absolute rainfall values forecast in some cases, the fact that the top value in re-forecasts was sometimes exceeded does show intrinsic forecast value. The Hong Kong event is an exception – here the forecast was not that extreme for that location (and indeed the corresponding ensemble mean was only 20 mm), yet the Hong Kong Observatory still registered its wettest 24 h period since 1889.

If a rainfall value denotes a very isolated peak, then extreme impacts can be less widespread, and the forecast error can be deemed acceptable. However, if values are not forecast and are more typical of a wider area encompassing several model grid boxes (as in the Hong Kong case), then the model is exhibiting more worrying error behaviour, on its own grid scales. For the top-ranked Greece event, the observation figure for the rainfall event on 5 September 2023 suggests that the extraordinary values >500 mm were relatively isolated, and that 200–300 mm, as predicted for Portaria, was more typical to the west. However, we should not underplay the societal impacts, which were exceptional and widespread for this case. Also, this is only a segment of what was a multi-day event in Greece.

Maximum 24 h rainfall in 9 km resolution re-forecast sets for June, July, August and September. This is based on about 15,000 realisations with IFS Cycle 48r1, equivalent to the yellow boxes on the scatterplot. Sampling issues make the raw product very noisy, so conservative interpolation has been applied to smooth to 144 km resolution for this plot. This does reduce some genuine topography-related peaks, although that tends to be more of an issue outside of summer.

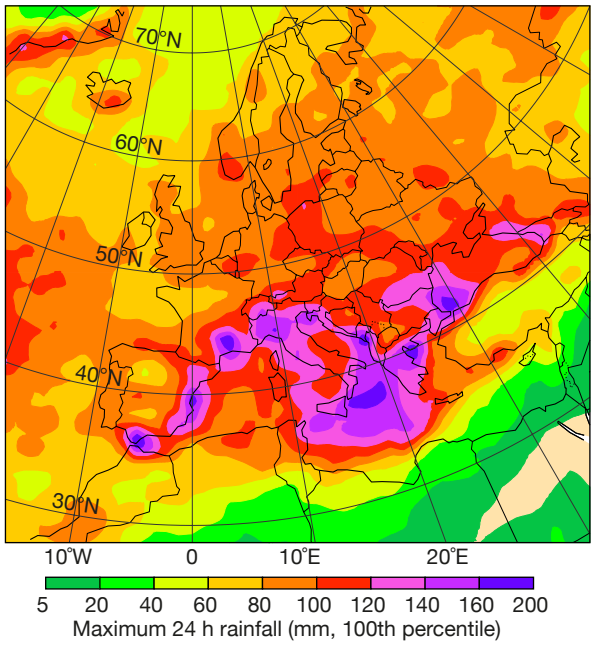

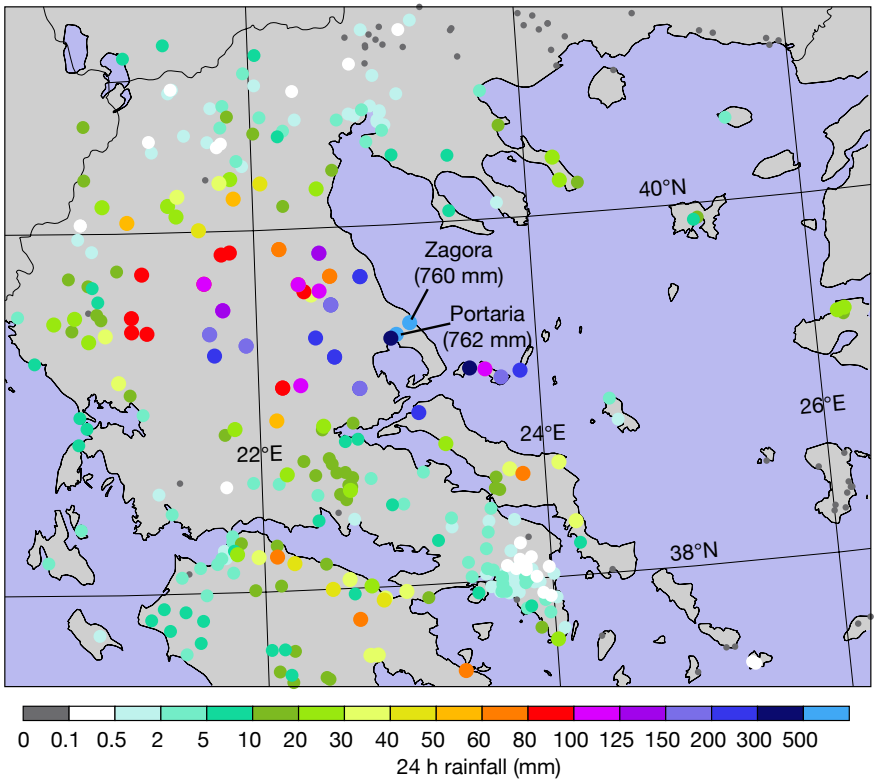

24 h rainfall for 5 September 2023. The Portaria value represents a new all-time Greek record. Many thanks to Kostas Lagouvardos (National Observatory of Athens/Institute for Environmental Research) for providing supplementary, quality-controlled data for the region of Thessaly in central Greece that includes the two labelled values.

Possible remedies

So how can we address the IFS shortfalls in representing local rainfall extremes? Currently one can use post-processed ecPoint output, that aims to predict values, probabilistically, at rain gauge scale. Presently only 12 h totals are available, although 6 h and 24 h fields are in development. Or one can use higher-resolution limited-area ensembles, which are quite commonplace in Europe. In the longer term, ECMWF will run higher-resolution global models operationally, and a key 'testbed' for this is the experimental (4.4 km) runs from the EU-funded Destination Earth (DestinE) initiative. These have been trialled on many of the cases described here, and first results look quite promising.

AIFS: a new ECMWF forecasting system

Simon Lang, Mihai Alexe, Matthew Chantry, Jesper Dramsch, Florian Pinault, Baudouin Raoult, Zied Ben Bouallègue, Mariana Clare, Christian Lessig, Linus Magnusson, Ana Prieto Nemesio

There has been substantial progress recently in the realm of data-driven weather forecasting. Big technological companies like Google, Huawei and Nvidia have built purely data-driven weather forecasting models. These models outperform leading physics-based global numerical weather prediction (NWP) models in many of the standard forecast scores, such as root-mean-square error (RMSE) and Anomaly Correlation Coefficient (ACC) for geopotential height at 500 hPa. They are trained on historical weather data, usually a subset of ECMWF's ERA5 reanalysis dataset, and they rely on traditional NWP analyses as initial conditions when producing a forecast.

To better understand and explore the machine learning (ML) technologies underpinning these models, ECMWF decided to implement a data-driven forecast model, the **A**rtificial **I**ntelligence/Integrated **F**orecasting **S**ystem (AIFS), a homage to ECMWF's Integrated Forecasting System, the IFS. The AIFS is underpinned by a toolkit (Anemoi, Greek: 'Winds'), which provides high-performance building blocks and pipelines to create and train massively parallel AI-driven forecast models.

AIFS products are now available on ECMWF's OpenCharts alongside charts of the IFS and other machine learning models (https://charts.ecmwf.int/).

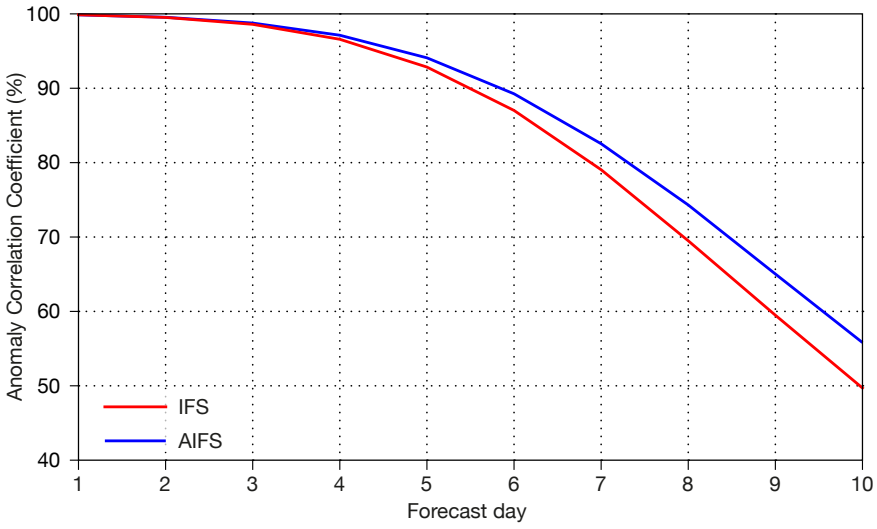

AIFS forecast skill. We show the northern hemisphere Anomaly Correlation Coefficient (ACC) for geopotential height at 500 hPa of IFS forecasts (red, dashed) and AIFS forecasts (blue) for 2022. Higher values indicate better skill.

Field	Level type	Input/Output
Geopotential, U component of wind, V component of wind, vertical velocity, specific humidity, temperature	Pressure level: 50, 100, 150, 200, 250, 300, 400, 500, 600, 700, 850, 925, 1000	Both
Surface pressure, mean sea-level pressure, sea-surface temperature, 2 m temperature, 2 m dewpoint temperature, 10 m U component of wind, 10 m V component of wind	Surface	Both
Land-sea mask, orography, standard deviation of sub-grid orography, slope of sub-gridscale orography, insolation, latitude/longitude, time of day/day of year	Surface	Input

AIFS training data. The table provides an overview of AIFS inputs and outputs during training.

ECMWF's fully data-driven weather forecast model

There is currently a diverse set of deep-learning architectures being employed in the context of data-driven weather forecasts, e.g. vision transformers, neural operators, and graph neural networks (GNNs). We have decided to follow the approach of Ryan Keisler and Google DeepMind's GraphCast and implement a forecast system based on GNNs. One attractive property of GNNs is that they can learn from data on arbitrary grids, and this allows the AIFS to work directly with the native IFS reduced Gaussian grids.

Our toolkit has a modular design that allows for flexibility, such as future extensions or architectural changes to the AIFS. It relies on the Pytorch machine learning framework, and Pytorch Geometric is used to implement the GNN architecture.

The version of the AIFS available at the time of writing is trained on a subset of the ERA5 reanalysis for 1979–2018 and fine-tuned on operational IFS data from 2019 to 2020. Pressure level fields and surface fields are used for training, together with forcing data, like time of the year and insolation. A complete list of AIFS inputs and outputs is given in the table. The input and output are currently at about one degree resolution.

Although they are still produced at relatively coarse resolution, AIFS forecasts show higher skill than IFS forecasts when measured by a range of standard forecast scores (an example is shown in the image). This is already in line with the current leading data-driven external models.

One area where resolution has a substantial impact is for surface parameters, such as 2 m temperature. As expected, for these variables the AIFS at a resolution of one degree is still behind the operational IFS configuration. First tests with higher-resolution variants of the AIFS show that large improvements are possible in this area.

Outlook

The first incarnation of the AIFS shows very promising results, replicating the rapid progress that has been made in the realm of data-driven AI weather models. We are now training a higher-resolution version of AIFS, which once tested will replace the current version on OpenCharts. An important next step will be to extend AIFS to create ensemble forecasts. Here, different avenues are possible, such as probabilistic training or exploiting generative AI architectures, like diffusion models. Work has already started to explore these options. Another interesting area of ongoing research is the coupling of data-driven models trained on NWP analysis to observational data, or even the training solely involving observations (see the feature article in this Newsletter).

Moving forward, a new ECMWF Member State pilot project on machine learning was recently approved. In this, Member States and ECMWF will work together to further develop data-driven forecasting methods and models, applied across a range of scales from global to local.

There has been rapid progress in the development of highly skilful data-driven weather forecast models, and we expect further advances soon.

ECMWF meets its representatives in 2023

Becky Hemingway, Julia Ioannou, Carsten Maass, Emma Pidduck, Tim Hewson, Matthieu Chevallier, Ahmed Benallegue

ECMWF Representatives in our Member and Co-operating States play a vital role in disseminating information, providing feedback to ECMWF, and managing users and the use of ECMWF products and services. In 2023, five meetings were held between ECMWF and Member and Co-operating State Representatives. In May, Catalogue Contact Points met, and the Security Representatives Meeting was held, both virtually. In October, the Computing Representatives met in person in Bologna as a side meeting to the high-performance computing (HPC) workshop. In November, a Co-operating States' User Forum was held for the first time, followed by the Meteorological User Forum for Meteorological Representatives; both were online. We now aim for all meetings to be held annually.

Representatives' meetings are an opportunity for ECMWF to present updates and discuss a variety of topics, and to get to know user issues in Member and Co-operating States. The meetings also invite attendees to share and discuss experiences from their own countries and provide an opportunity to network with fellow representatives. These meetings are one of many ways ECMWF engages with Member and Co-operating States, and we would like to thank the Representatives for the important role they play.

More information on each meeting can be found below.

Catalogue Contact Points (CCP) Meeting

The 2023 CCP Meeting was attended by 11 Member and Co-operating

Computing Representatives' Event. Attendees in person and online at the Computing Representatives' Event 2023 held in Bologna, Italy.

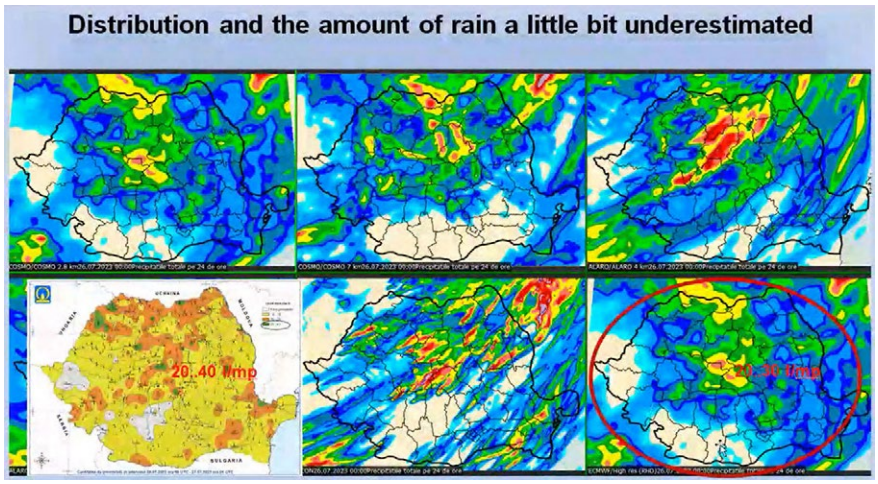

Meteorological User Forum. Meda Andrei (National Meteorological Administration, Romania) presented a summary of model performance vs. observations for precipitation during a recent event in Romania.

States. The meeting focused on Cycle 48r1 of ECMWF's Integrated Forecasting System (IFS), a new service charge model, and updates to licensing policies. Attendees provided useful and informative updates on data policies, licensing and provision in their organisations and countries. At the time of the meeting, Cycle 48r1 was near to implementation, so ECMWF colleagues stressed the importance of user testing of the new data configurations. Valuable discussions were had on applications and licensing.

Security Representatives' (SecRep) Meeting

The SecRep Meeting welcomed around 15 Member and Co-operating States and the European Space Agency (ESA) to review the status of security arrangements at ECMWF and within Member and Co-operating States and to discuss planned information security development. The topics discussed included the Zero Trust Security approach, which relates to the increase in remote working, and various matters linked to cybersecurity. Attendees appreciated the discussions and information shared.

Computing Representatives' Event

Twenty-three Computing Representatives attended the Computing Representatives Event 2023 held in person in Bologna, with an additional eight participating online. The event was held exceptionally in person as a side meeting to the HPC workshop. It provided an opportunity to showcase the Atos HPC to those who work alongside users.

Presentations were given by ECMWF staff covering computing services updates, future IFS model cycles, GRIB2 migration, data licensing and the Computing Representatives' role. Member and Co-operating States presented informative updates on work in their respective countries. This included Alex Deckmyn from Belgium, describing how the Royal Meteorological Institute of Belgium (RMI) now runs operationally in Bologna; Hans de Vries from the Netherlands, explaining how they are moving toward cloud computing; and Thomas Lorenzen from Denmark, providing an update on the United Weather Centre West (UWCW) supercomputer collaboration. In the afternoon, a session was held jointly with EUMETSAT on the European Weather Cloud (EWC), providing updates on the now-operational EWC and the role of Computing Representatives in this. The event afforded an excellent opportunity to discuss and learn about common challenges faced by many institutes, as well as to celebrate the longstanding connections that have formed as a result of this group.

Co-operating States' User Forum

A Co-operating States' User Forum was held for the first time in November 2023. The forum is the result of a request from the Advisory Committee of Co-operating States (ACCS) and provides a place for Co-operating States to discuss issues that are of direct relevance to them. More than 20 attendees from nine Co-operating States joined the meeting. Discussions included forecast products, product access and ECMWF membership. Davit Loladze from Georgia and Ilia Gospodinov from Bulgaria gave presentations on their use of ECMWF products. All attendees indicated that the forum was either somewhat useful or very useful, and all wanted future meetings. The Co-operating States' User Forum will become an annual meeting.

Meteorological User Forum

The Meteorological User Forum is an annual meeting for ECMWF Meteorological Representatives from all Member and Co-operating States. Twenty-one attendees joined the meeting, where a variety of topics were presented and discussed. These included new forecast products; ecCharts and OpenCharts; machine learning; IFS Cycle 48r1; IFS Cycle 49r1; the planned ERA6 reanalysis; the Using ECMWF Forecasts (UEF) event; and Member and Co-operating State engagement and visits. Thomas Schumann from the German Meteorological Service (DWD) and Meda Andrei from the Romanian National Meteorological Administration (ANM) both provided insightful presentations, including issues with ECMWF forecasts, which will be investigated in more detail. Feedback on the meeting was positive, with one attendee commenting: "Thank you very much for all the great presentations and discussions!" All participants welcomed the range of updates and topics covered.

ECMWF heating rates support PHILEAS aircraft campaign

Jens-Uwe Grooß (Forschungszentrum Jülich)

The German research aircraft HALO has provided valuable contributions to research into the effects of the Asian Summer Monsoon and wildfires in Canada on climate. Between August and October 2023, HALO was involved in the PHILEAS mission. A team of researchers coordinated by Forschungszentrum Jülich and Johannes Gutenberg University Mainz (Germany) has been investigating the impacts of the Asian Summer Monsoon on global climate. Heating rates from ECMWF operational forecasts were used to help determine the best possible locations for the flight paths. The wealth of exceptional data collected will allow profound insights into how the Asian Summer Monsoon and so-called pyroconvection transport airborne pollutants. With regard to the latter, large-scale fires of the type seen in Canada generate powerful convection currents and also pyrocumulonimbus or thunderstorm clouds.

Measurement flight start of HALO. Various air inlets are visible at the top, and the belly pod with the remote sensor GLORIA can be seen below the fuselage. (Copyright: Andreas Minikin/DLR)

Two campaign phases

The main objective of this PHILEAS campaign was to study the effects of the Asian Summer Monsoon on climate. Convective systems tend to predominate vertical transport in this massive weather system. They can convey highly contaminated air from the near-surface atmosphere in Southeast Asia to elevations of up to 15 kilometres in the atmosphere. From there, the polluted air spreads to the west into the area above the Eastern Mediterranean and to the east over the Pacific.

During the first measurement phase from early to mid-August, the researchers were able to analyse monsoon air containing a large proportion of the pollutants present over the Eastern Mediterranean, reaching locations above Israel and Jordan. In the second campaign phase involving flights from Anchorage in Alaska, the transport of contaminated air over the Pacific, Alaska, and Canada was investigated. This was the first time that scientists could study in

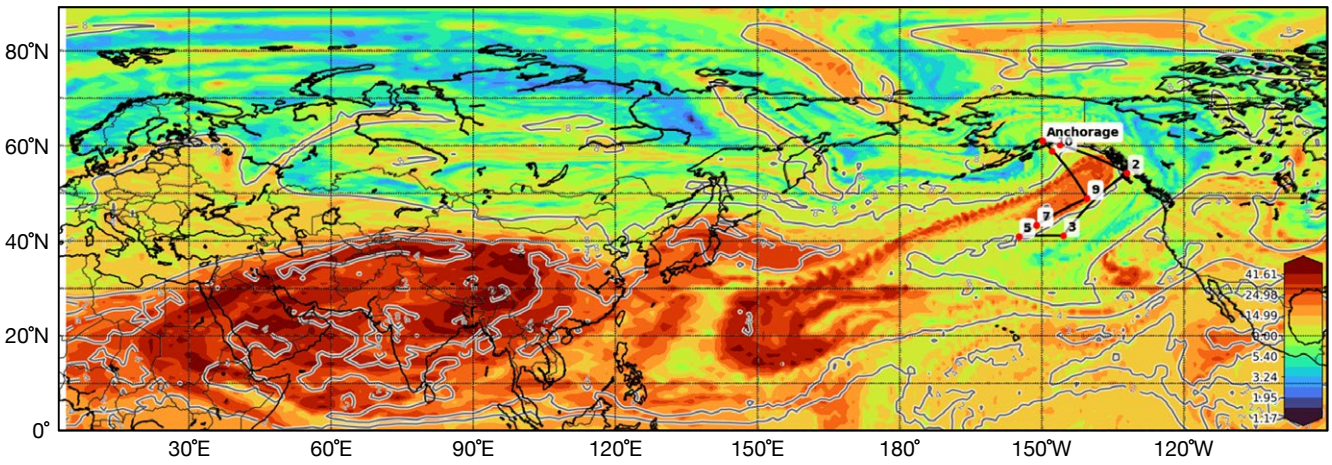

Flight planning chart. Scientific flight planning by the Mission Support System (MSS) from 14 September 2023, displaying CLaMS model results for 17 September, namely the fraction of air originating from the surface in South Asia. The chart thus shows the likely locations of contaminated air masses originating from South Asia, together with the planned flight track of the HALO aircraft from Anchorage. (Copyright: Martin Riese/Forschungszentrum Jülich)

detail an extensive quantity of polluted monsoon air at higher latitudes, in this case as high as the lower stratosphere. For example, on successive days the same air masses could be monitored and analysed. In Anchorage, there also was an opportunity to assess the impact of wildfires in Canada. These were particularly severe in the Northwest Territories around Yellowknife. Measurements were taken near the fire sources, with pyroconvection currents taking the products of combustion up as far as the stratosphere.

ECMWF's contribution

In order to achieve most successful research flights, a sophisticated planning procedure is necessary, as it is not trivial to determine the best possible locations for a flight path. For that, the Chemical Lagrangian Model of the Stratosphere (CLaMS) of Forschungszentrum Jülich among others was used in forecast mode, employing ECMWF operational forecasts. For precisely modelling the vertical velocities in CLaMS, the heating rates (via the ttpha variable, which is the temperature tendency due to model physics) from ECMWF operational forecasts were needed. They had thankfully been recently made available. The flight planning figure demonstrates the locations of air masses originating from the Asian Monsoon anticyclone, simulated using artificial model tracers that mark the airmass origin.

Initial results of the analysis of the data should be available soon, but a detailed analysis of the wealth of data will take much longer as it will require considerable time to determine the effects on climate using complex associated modelling.

How did ECMWF seasonal forecasts perform for the European summer of 2023?

Antje Weisheimer

ECMWF's global SEAS5 operational seasonal forecast for the months of June, July and August (JJA) 2023, initialised on 1 May 2023, was dominated by warm sea-surface temperatures (SST) in the tropical Pacific, which marked the onset of the current El Niño event. SEAS5 accurately predicted the warming of the central and eastern equatorial Pacific, along with many of its global teleconnections driven by the large-scale shift of the Walker circulation in the tropics.

Well-predicted El Niño–Southern Oscillation (ENSO) teleconnections include drier-than-normal conditions over the maritime continent, India and portions of Australia, the relatively dry and warm conditions over Central America and the dry season across large parts of South America.

In the northern extratropics, summer seasonal predictions are, in general, highly uncertain due to smaller magnitudes of the anomalies, overall reduced variability, and the absence of robust dynamical drivers. While warm near-surface temperature anomalies were correctly predicted over many land areas of the northern hemisphere, forecasting the atmospheric circulation proved more difficult.

Conditions over Europe

Over the North Atlantic, pronounced negative sea-level pressure anomalies extended from the east coast of the US across the ocean towards Ireland, Britain, and Scandinavia, according to ECMWF's ERA5 reanalysis (top-left panel). The eddy-driven jet over the North Atlantic shifted southward, leading to a band of stronger westerly winds at 850 hPa from western Europe to the Baltic Sea (middle-left panel). These circulation anomalies describe the negative phase of the so-called Summer North Atlantic Oscillation (SNAO), which is distinctly different from the winter NAO. The unsettled and wet weather experienced across western, northern and central Europe during July and August directly resulted from the negative SNAO circulation anomaly.

SEAS5 successfully generated ensemble mean forecasts of surface pressure and zonal wind anomalies that captured the observed southward shift of the jet over the North Atlantic (top- and middle-right panel). However, the model struggled to forecast the eastward extension of the jet into Ireland, Britain, and Scandinavia. Instead, the ensemble mean shows a weak signal of large-scale blocking over the North Sea and Scandinavia with easterly wind anomalies and suppressed precipitation.

To further investigate the performance of SEAS5, we define a simple SNAO index as the area-mean seasonal mean sea-level pressure anomaly over the box 45°N–65°N/15°W–15°E and analyse the ensemble distribution of the index (bottom-left panel).
In comparison to the SEAS5 long-term climatological distribution during the 1993–2016 hindcast period, the forecast ensemble for JJA 2023 is slightly shifted towards more positive values. However, the ensemble spread is considerable, spanning a wide range of negative and positive values for JJA 2023. The observed negative index in ERA5 (red stars in the bottom-left panel) falls at the lower end of the climatological ERA5 distribution and is encompassed within the SEAS5 forecast distribution, despite its overall shift towards positive SNAO values.

The seasonal mean circulation anomalies outlined above mask some intriguing sub-seasonal developments: ERA5 shows that May and June 2023 saw a strong blocking over Scandinavia, followed by large but opposite anomalies in July and more typical conditions in August (see the red stars in the bottom-right panel). SEAS5, however, failed to predict the distinct shift from blocking to a more westerly flow in July. Instead, it exhibited a tendency to persist the blocked flow conditions from early May through June and July. Consequently, the overly persistent model forecast led to a positive seasonal mean signal in contrast to the observed negative anomaly.

The Copernicus Climate Change Service (C3S) implemented by ECMWF

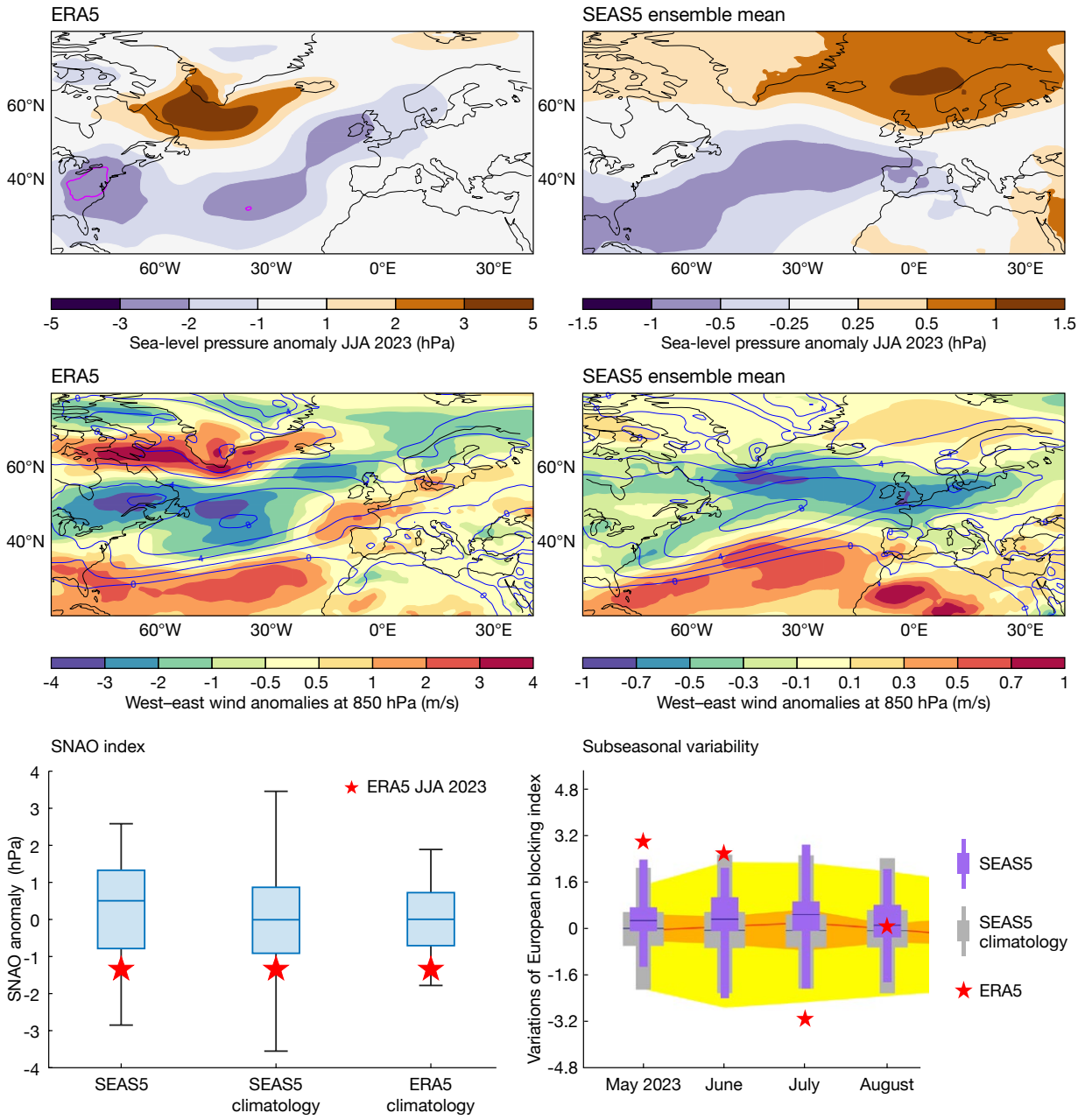

Performance of SEAS5 for the 2023 European summer season (JJA). The top two panels show mean sea-level pressure anomalies over the North Atlantic and Europe in ERA5 (left) and in the ensemble mean of SEAS5 for the forecast started on 1 May 2023 (right). The magenta line in the left-hand panel indicates where the anomaly exceeds three standard deviations during the reference period. The middle panels show west–east wind anomalies at 850 hPa (colour shades) and climatological mean winds (contours) in ERA5 (left) and SEAS5 (right). The bottom left-hand box-and-whisker plots are of the distributions of the SNAO index in the SEAS5 forecast, in the SEAS5 hindcast climatology, and in the ERA5 climatology. The boxes represent the interquartile ranges of the central 50% of the data. The red star highlights the ERA5 anomaly for JJA 2023. The bottom right-hand plot shows the climagram of monthly variations in SEAS5 forecast distributions of the European blocking index in purple, contrasting with the grey SEAS5 climatological hindcast distributions. The middle terciles of the observed climatology are represented in orange, while the upper and lower terciles of the observed climatology are denoted in yellow. The red star highlights the ERA5 anomalies for 2023. All anomalies are calculated with reference to the period 1993–2016, except for the climagram, which uses the period 1981–2010.

publishes seasonal forecasts from a range of models. Similar to SEAS5, most other models also fell short in accurately predicting the circulation patterns and, consequently, the precipitation signals over Europe for the summer of 2023.

Tropical Atlantic SSTs

The SSTs across the tropical and subtropical North Atlantic exhibited an unusual warm signal in JJA 2023, which was well reproduced in the SEAS5 forecast. Warm SSTs favour the development of tropical storms and hurricanes in the Atlantic basin and thus counteract the tendency to suppress tropical storm formation over the tropical Atlantic during El Niño events. The observed and SEAS5-predicted above-average tropical cyclone season in the North Atlantic (19 observed and 17 predicted compared to an average of 14) supports the hypothesis that the warm SSTs dominated this season, outweighing the impact of the ongoing El Niño.

A daily forecast with the prototype global Extremes Digital Twin of Destination Earth

Benoît Vannière, Irina Sandu, Peter Düben, Michael Maier-Gerber, Josef Schröttle, Jasper Denissen

Since 21 August 2023, a prototype of the global component of the Weather-Induced Extremes Digital Twin, developed at ECMWF as part of the Destination Earth initiative of the European Commission, has been producing daily forecasts on ECMWF's Atos supercomputer at a resolution of 4.4 km. By comparing these forecasts with ECMWF's operational forecasts at 9 km resolution, we can assess the additional benefits of the kilometre-scale resolution to predict extreme weather events. Here, we describe some successes and challenges we have seen over the last four months. The example of tropical cyclones will provide some evidence of the capabilities of forecasts at a resolution of 4.4 km.

The global Extremes Digital Twin

Destination Earth (DestinE) aims to create a digital twin of the Earth to enhance Europe's ability to respond and adapt to extreme weather and climate change. The initiative is implemented by ECMWF, ESA and EUMETSAT under the leadership of the Directorate-General Communications Networks, Content and Technology (DG CNECT) of the European Commission. ECMWF oversees the development of the first two high-priority digital twins, on Climate Change Adaptation and Weather-Induced Extremes, and of the Digital Twin Engine.

The Weather-Induced Extremes DT (or the Extremes DT) will support decision-making for a rapid response to meteorological, hydrological and air quality extremes, on a timescale of a few days ahead. It will have both a global component developed at ECMWF, run regularly to produce simulations at resolutions of a few kilometres for four to five days ahead, and a regional component, implemented in an activity procured by ECMWF from a large partnership led by Météo-France. It will be possible to configure and activate this regional component on demand, allowing users to zoom-in on extreme events happening across Europe with simulations at even higher resolutions (a few hundred metres).

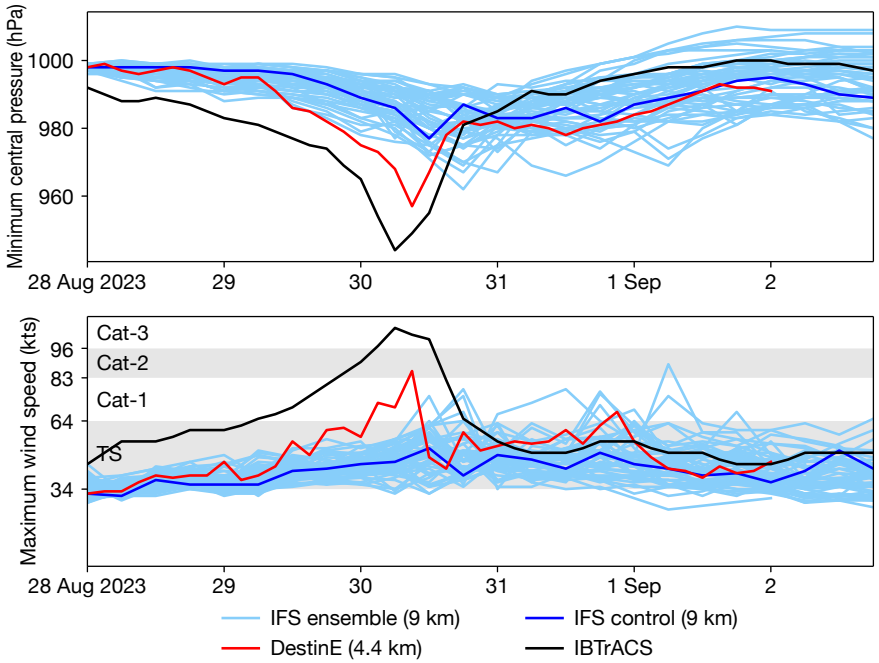

TC Idalia forecasts. Time evolution of mean central pressure (top) and maximum wind speed (bottom) for TC Idalia in the IFS ensemble members and the IFS control forecast, both at 9 km resolution, and in the DestinE global Extremes DT forecast at 4.4 km resolution. All runs are initialised on 28 August 2023, 00 UTC, and compared against IBTrACS observations.

Since the beginning of DestinE in December 2021, ECMWF has worked on developing a prototype of the global component of the Extremes DT. The prototype developed so far builds on the operational version of ECMWF's Integrated Forecasting System (IFS) (Cycle 48r1). However, it advances that version by increasing the horizontal resolution from 9 km to 4.4 km; by tailoring the representation of physical and dynamical processes to km-scale resolutions; and by adding novel simulated satellite imagery capabilities, specifically for visible channels.

Currently, the prototype global Extremes DT is initialised from the ECMWF operational analysis also used for ECMWF operational forecasts at 9 km resolution. The simulations are coupled, but for now the resolution of the NEMO ocean model is the same as in the operational forecasts (0.25 degrees). The resolution of the ECWAM wave model is 0.05 degrees compared to 0.125 degrees in the operational forecasts.

Work is also ongoing to integrate impact-sector elements in the global Extremes DT, notably for river discharge and inundated areas and a prognostic treatment of selected aerosol species. In addition, we are working on improving the DT initial conditions by using more continuous and higher-resolution data assimilation and through a better use of high-resolution observations.

First results

Initial simulations performed at 4.4 km, with the operational

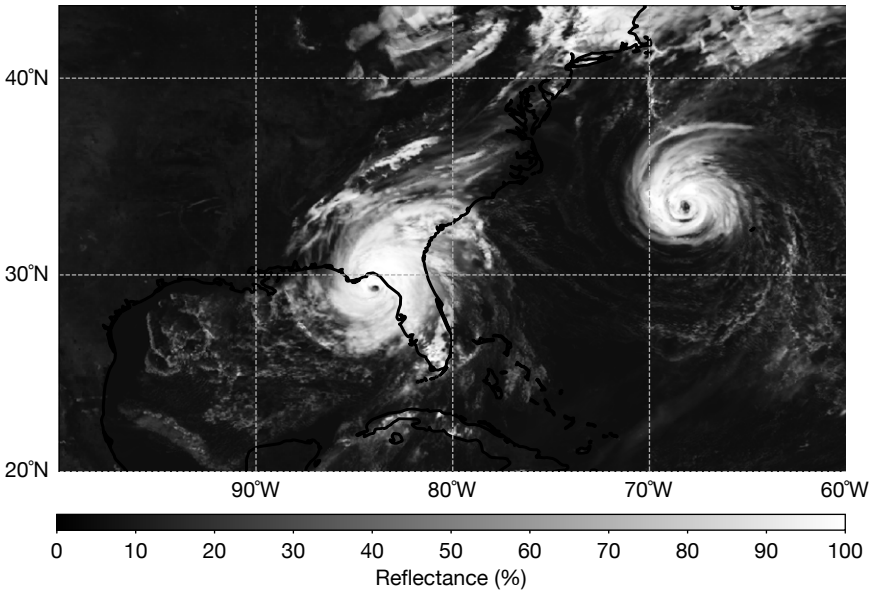

Simulated visible image. The image shows visible reflectance over the Gulf of Mexico and the Caribbean in the 0.64 µm spectral band for a 36 h forecast with the global Extremes DT, initialised at 00 UTC on 29 August 2023.

configuration of the IFS apart from the resolution, showed an improvement in the prediction of tropical cyclone intensity and of orographic precipitation maxima. However, the large-scale circulation scores were degraded, and work was needed to improve the model configuration used for kilometre-scale simulations. Notably, extra-filtering of the model mean orography was needed at small scales to reduce gravity waves that the hydrostatic model cannot simulate well. The model time-step was also decreased to increase model accuracy. This optimised configuration of the IFS was used to demonstrate the capability to produce daily forecasts with the prototype global Extremes DT.

Five-day deterministic forecasts at 4.4 km resolution have been run daily (at 00 UTC) with this prototype since August 2023. An offline suite is also run with the hydrological CaMa-Flood model, forced with the global Extremes DT to produce river discharge and inundated areas at 3 arcmin resolution (~5 km). ECMWF analysts can now compare the DestinE simulations at 4.4 km with ECMWF operational forecasts at 9 km on a daily basis.

Successes include the prediction of the intensification of tropical cyclone Idalia. This happened just a few days after the daily simulations with the global Extremes DT were initiated. Idalia made landfall on 30 August 2023 in Florida, with hurricane-force wind. While the control of ECMWF's operational ensemble forecasts did not even manage to predict that the cyclone would reach category 1, the prototype DT predicted a category 2 when the forecast was initialised on the 28 August 00 UTC (see the forecast plots). It successfully predicted category 3 24 hours later, in close agreement with the observed IBTrACS intensity. Hurricane Franklin occurred simultaneously to the north-east of Florida over the Atlantic. Simulated satellite images of reflectance clearly show the narrow eye structure of Idalia and Franklin predicted by the prototype DT, as well as fine-scale structure in the spiralling cloud bands surrounding both hurricanes (see the simulated visible image).

However, we found that the increased resolution does not always lead to an improved prediction of tropical cyclones. For example, tropical cyclone Otis, which made landfall near Acapulco on 25 October 2023, was a major forecast bust. Its rapid intensification from tropical storm intensity to category 5 in less than 24 hours was missed by all operational models. Unfortunately, the prototype global Extremes DT also fell short of predicting the event, failing to even reach category 1.

Planned improvements

The failure to properly forecast Otis could be due to a combination of factors that other activities within Destination Earth have the potential to address. Indeed, the difficulty of initialising a weak and small tropical depression with a coarse resolution analysis might have played a crucial role in the forecast failure. We are working on a higher-resolution 4D-Var system assimilating more observations with the potential to provide improved forecast initial states at higher resolutions. We are also actively exploring new physics for convection to address errors in the representation of mesoscale convective systems, which tend to be too weak in the IFS at a resolution of both 9 km and 4.4 km. The intense convective activity embedded in the tropical depression from which Otis developed could have played a pivotal role in the onset of the event.

Work is continuing to produce daily simulations with the global Extremes DT on EuroHPC systems. Simulations will first be performed on the LUMI supercomputer in Finland, and then on Leonardo in Italy. Work is also ongoing to connect the Extremes DT with the DestinE data lake, implemented by EUMETSAT, and the DestinE core platform, implemented by ESA, which will allow users to access the data of DestinE DTs. The objective is to have all these essential building blocks in place to demonstrate production capability for the Extremes DT on EuroHPC at the end of Phase 1 in June 2024, when the DestinE system will open to users.

In parallel, work to continuously advance the global extremes DT will continue through the remainder of Phase 1 of DestinE and in Phase 2, by improving the representation of physical processes, by activating selected prognostic aerosol species, and by enhancing the accuracy of the initial conditions for Earth system components.

Probabilistic clear-air turbulence

Peter Bechtold, Cihan Sahin, Axel Bonet, Sándor Kertész

Clear-air turbulence (CAT) is the main weather threat to civil aviation at cruising level in the lower stratosphere. It is generated from shear instabilities near jet streams and boundary-layer inversions, thermal instabilities, and breaking small-scale gravity waves. The latter phenomenon is generated predominantly above orography and convective clouds. As requested by users, a CAT parameter has been developed together with the Deutsches Zentrum für Luft und Raumfahrt (DLR) in Germany, and it has now become a fully probabilistic product.

CAT was originally made available from ECMWF's high-resolution forecast in October 2021, with the introduction of Cycle 47r3 of the Integrated Forecasting System (IFS). It is based on the Eddy Dissipation Rate (EDR) ($m^{2/3}s^{-1}$), which is the international standard measure of turbulence in aviation (see ECMWF Newsletter No. 168). CAT has been provided on specific flight levels in ecCharts since then, as requested by our Member States, and specific EDR thresholds are generally used to distinguish between light, medium and severe turbulence.

Probabilistic CAT

Free atmospheric turbulence is an intermittent and rare process: it occurs only 1–3% of the time as derived from research aircraft measurements. A probabilistic approach can help to judge the significance and to obtain reasonably smooth fields. With the introduction of IFS Cycle 48r1 and the availability of a high-resolution (9 km) 51-member ensemble since June 2023, we have extended the graphical processing of CAT to turn it into a fully probabilistic product. This required, however, extensive optimisation of the post-processing suite that interpolates the CAT fields from model levels to height levels and then to flight levels. A set of probability thresholds (probability of CAT exceeding 0.1, 0.15, 0.25, 0.32, 0.45 $m^{2/3}s^{-1}$) is then computed for each flight level. We can now provide the highest resolution probabilistic CAT product worldwide in

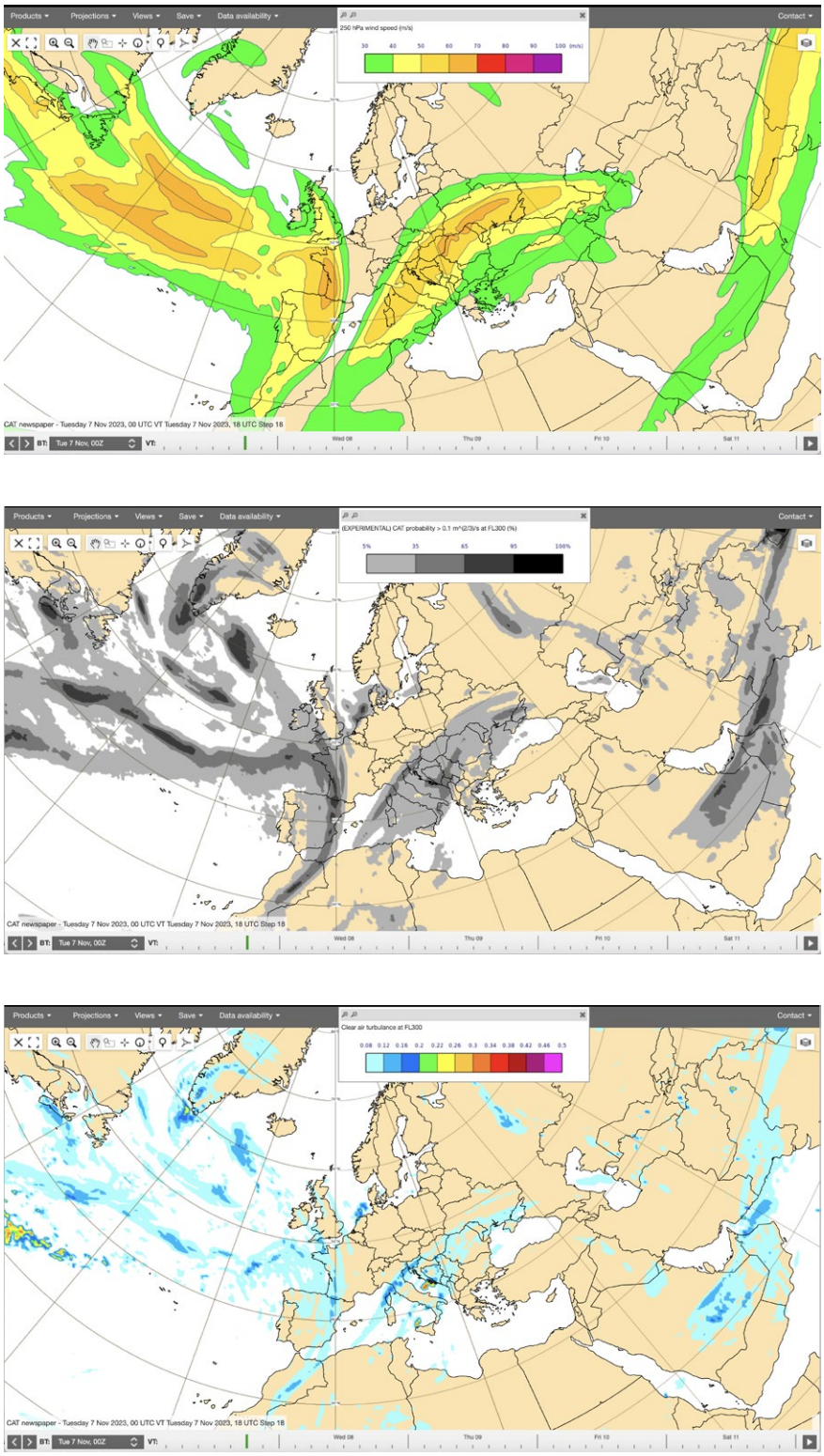

CAT in ecCharts. The image shows 18-hour forecasts of 250 hPa wind isotachs over Europe from 7 November, 00 UTC (top), the probability of CAT to exceed 0.1 $m^{2/3}s^{-1}$ at Flight level 300 (~9,200 m) (middle), and CAT at Flight level 300 from the HRES suite (bottom). In the ecCharts interface, these parameters can easily be overlayed, and any region globally can be considered at different zoom settings.

terms of vertical and horizontal resolutions and ensemble size. The illustration shows three aspects of an 18-hour forecast from 7 November 2023 at 00 UTC: the wind field at 250 hPa; the probability of CAT to exceed 0.1 $m^{2/3}s^{-1}$; and CAT from the high-resolution (HRES) suite, which has the same 9 km resolution as the ensemble forecast introduced in June 2023. Regions of light to moderate turbulence can be seen in the fringes of the jets over the central Atlantic, western Europe and northern Italy. There is also orographically enhanced turbulence over the Dalmatian islands, off Sicily, and off the southern tip of Greenland.

Both CAT and high-resolution probabilistic CAT products are accessible in ecCharts. Editing these layers will let users choose the flight level and, in the case of the probabilistic CAT layer, the probability threshold to be visualised.

Other products

Active users of ECMWF's CAT forecasts include the Hungarian Meteorological Service (OMSZ) and the Croatian Meteorological and Hydrological Service (DHMZ), from whom we receive valuable feedback for improvement. Other available CAT products worldwide include the Graphical Turbulence Guidance (GTG), which was developed at the US National Center for Atmospheric Research (NCAR). This is used by the US National Oceanic and Atmospheric Administration (NOAA) weather service and also by the UK Met Office and the Korean Meteorological Administration. Contrary to the ECMWF product, where CAT is computed online during the forecast, the GTG is a post-processing package that computes a large set of turbulence-related parameters and provides adapted graphical output. A similar procedure to the one used for the GTG has also been adopted by Météo-France, although its CAT product also includes the turbulent kinetic energy as a parameter. Finally, the CAT provided by the German Meteorological Service (Deutscher Wetterdienst) is based on summing over all sources of turbulent kinetic energy as available from the ICON model. It is therefore the most similar quantity to the ECMWF CAT, which is based on a method including available physical sources of turbulent dissipation.

Monitoring and climatology

Compared to other available and mature aviation products as mentioned above, the ECMWF ensemble CAT provides complementary guidance as it is close to turbulent dissipation in the IFS model. The introduction of stochastic parameter perturbations in the upcoming IFS Cycle 49r1 will further improve the sampling. However, the product could benefit from further calibration, and we aim to further evaluate CAT with available observations. Unfortunately, aircraft observations of EDR are difficult to obtain and remain the property of the individual airlines. We therefore plan, in collaboration with colleagues from Yonsei University (Seoul, South Korea), to pursue the validation by deriving EDR values from high-resolution radiosonde data using the well-known Thorpe method in turbulence.

A climatology of post-processed CAT has recently been established by a group at Seoul National University for ECMWF's ERA5 reanalysis, using the GTG software. The new ECMWF CAT will be available in ECMWF's upcoming ERA6 reanalysis on pressure levels. This will facilitate a new climatology of CAT and make it easier to monitor its evolution in a changing climate.

New software libraries for ORAS6 ocean reanalysis

Domokos Sármány, Kristian Mogensen, Mirco Valentini, Razvan Aguridan, Philipp Geier, James Hawkes, Simon Smart, Tiago Quintino

Global reanalyses provide the most complete picture currently possible of past weather and climate, because they make use of all available observations combined with the best short-range output from the most recent forecasting systems. Here we describe a new set of software libraries, called MultIO, that has been developed so that ECMWF's future ORAS6 ocean reanalysis can feed efficiently into its next atmospheric reanalysis, ERA6.

MultIO

Reanalyses are widely used in climate-assessment studies and, more recently, in training weather-forecasting models based on machine learning. ECMWF has a long history of producing both atmospheric and ocean reanalyses, with the latest atmospheric reanalysis being the fifth-generation iteration, called ERA5, and the latest ocean reanalysis being ORAS5. It is now preparing for the next generation of reanalysis, ERA6, which will also include ocean data from the next-generation ocean reanalysis, ORAS6.

As a result, it was imperative that the ocean model would be able to archive data in ECMWF's archival system, MARS, and that it would be able to do so efficiently. In an early evaluation, we deemed the existing output library used by recent versions of the NEMO ocean model, XIOS, insufficient for this purpose because of its tight coupling to the netCDF data format. Instead, we have developed MultIO, a set of software libraries that offer two related, but distinct functionalities:

- An asynchronous I/O-server to decouple data output from model computations.
- User-programmable processing pipelines that operate on model output directly, accessing data while they are still in memory, and thus

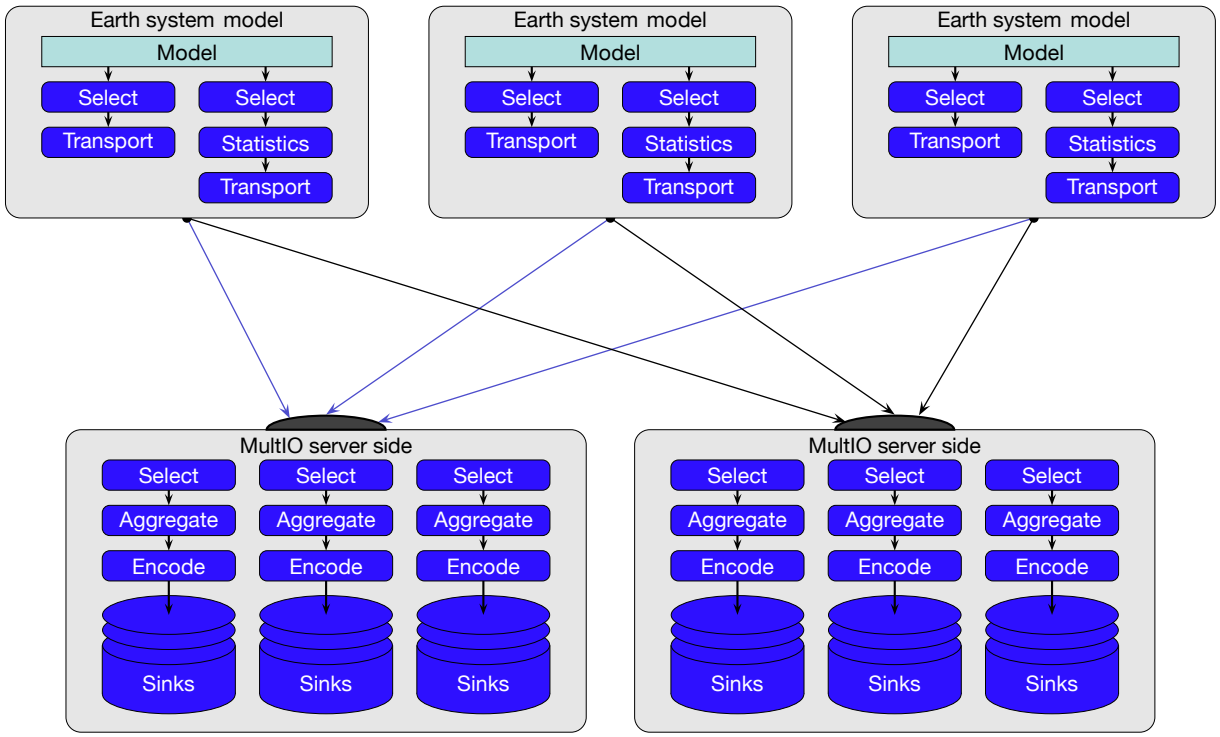

Server design. The figure provides an overview of MultIO's pipelining and I/O-server design. Earth system models, such as a coupled atmosphere–ocean system, are geographically distributed. The aggregation of distributed fields into global fields takes place on the 'server side'. MultIO offers post-processing in its pipelines both on the 'model side' and the 'server side'.

reducing the storage I/O operations that are required for some of the most frequent post-processing tasks.

MultIO is a metadata-driven, message-based system. This means that the I/O-server and processing pipelines fundamentally handle and operate on discrete packets of data, self-described with attached metadata, called messages. The metadata attached to each message drive the behaviour of the I/O-server, the data-routing decisions, and the selection of actions. The type and volume of post-processing may be controlled by setting the message metadata via the Fortran/C/Python APIs, and by configuring a processing pipeline of actions. The first figure shows an overview of the pipelining and I/O-server design.

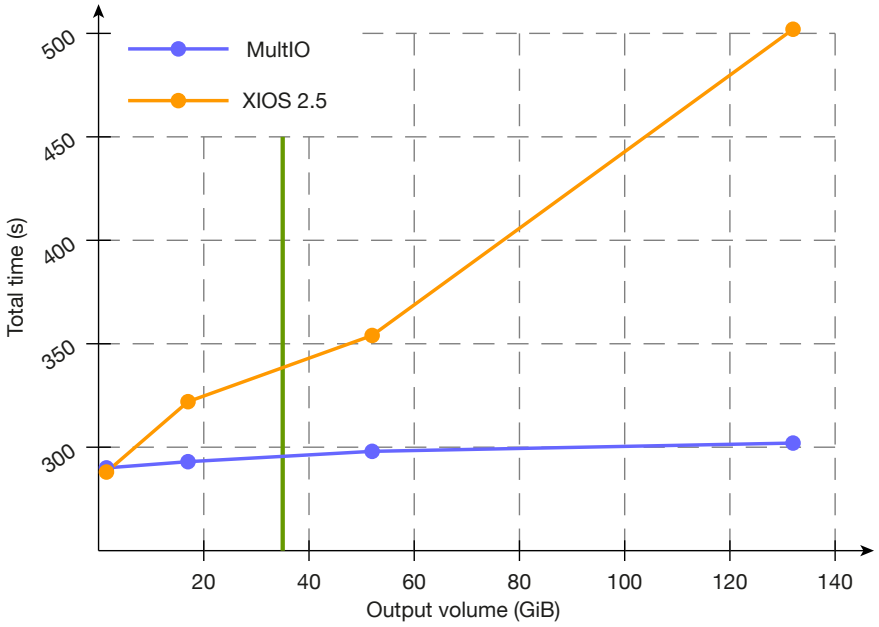

MultIO vs XIOS. Comparison of MultIO with XIOS 2.5 for different throughput volumes of a single five-day, one-ensemble-member assimilation loop. The vertical green line indicates an approximate volume for production.

MultIO's roles in achieving the aims of ORAS6 are three-fold:

- Aggregating horizontal global fields from distributed data.
- Computing temporal means from data at time-step regularity.
- Injecting the metadata information required for encoding all necessary fields in a GRIB2 format approved by the World Meteorological Organization (WMO), and encoding the data by calling the 'ecCodes' library.

The data governance and curation process has also been a crucial and independent part of the overall work. The process has resulted in around 90 new ocean parameters, approved by the WMO.

Pre-production evaluation

MultIO will enter production as the engine for model output for ORAS6 in early 2024. This will, in turn, feed

into the ERA6 production runs. The nature of ocean reanalysis is that many small or medium-sized data assimilation trajectories are executed on the high-performance computing system, rather than a few large runs. Although the actual details for production are still to be decided, the following is expected to be close to the final configuration: quarter-degree (eORCA025) ocean grids; thousands of five-day assimilation loops; 11 ensemble members; 300 compute tasks per member; 20 I/O tasks per member. With this topology, a single loop with one ensemble member takes around five minutes, but this may vary with output volume.

The MultIO vs XIOS graph shows the execution times of a single assimilation trajectory with increasing throughput. The likely production output volume is shown by the green vertical line. The execution time increases gently as data is output using MultIO, making simulation runs feasible even at throughput far exceeding what is planned for production. By comparison, we include the equivalent timings when data is output using XIOS, a popular choice among NEMO users. Although performance would still be acceptable in the likely production configuration, the cost would quickly become prohibitive for higher output volumes. This suggests that XIOS would be unsuitable for time-critical runs of coupled models.

Outlook

MultIO is currently able to output ocean parameters required for production in GRIB2 format. However, if research experiments require a wider range of parameters, there is an option to output netCDF format via XIOS, or even output both GRIB2 and netCDF simultaneously using both MultIO and XIOS. In the future MultIO is likely to be extended to support netCDF output directly, as part of an international collaboration. Work is also ongoing to replace the IFS's own Fortran I/O-server with MultIO for all model output.

Multi-party desert dust study delivers exciting results

Angela Benedetti (ECMWF), Emmanouil Proestakis, Vassilis Amiridis (both National Observatory of Athens), Maria Gonçalves, Carlos Pérez García-Pando, Joan Llort (all Barcelona Supercomputing Centre)

The multi-party 4D-Atlantic Dust & Ocean Modelling & Observing Study (DOMOS), funded by the European Space Agency (ESA), ran over two years from September 2021 to 2023 and delivered unique datasets and studies related to the dust cycle and its connections with atmospheric processes as well as ocean biogeochemistry. Desert dust is one of the most abundant aerosol types. As such, it is an important weather and climate forcer via its impact on solar-reflected radiation and Earth's emitted thermal radiation. Dust radiative processes can also affect the static stability of the atmosphere and might play a role in the development of cyclonic circulation. In addition, dust is the primary source of soluble iron. This is a necessary nutrient to produce tiny phytoplankton organisms, thought to be responsible for the absorption of atmospheric CO_2 connected to anthropogenic activity into the ocean.

The DOMOS consortium was formed by six partners: the Barcelona Supercomputing Center (BSC), the National Observatory of Athens (NOA), the Norwegian Meteorological Institute (MetNo), the University of Cologne, the Royal Netherlands Institute for Sea Research (NIOZ), and ECMWF (the coordinator).

Dust, dust everywhere...

The project delivered a new satellite-based dataset of dust optical depth and dust deposition over the Atlantic basin for the period 2007–2020 (see the first illustration), which has been evaluated against existing deposition datasets. The product is based on the LIVAS (LIdar climatology of Vertical Aerosol Structures) pure dust dataset, which provides profiles of dust concentrations derived from CALIPSO lidar measurements. The DOMOS-LIVAS deposition dataset shows an overestimation compared to ground-based, sparse measurements. This is possibly the result of assumptions that are made on particle size and dust scattering properties. More observations, such as the Aeolus and upcoming EarthCARE lidar observations, are needed to extend the product in time and to improve its accuracy. The project also showed the need for independent observations for the evaluation of satellite-derived products. Moored buoys and ship observations in open ocean areas are key to this calibration and evaluation activity, as they are deployed in areas where ground-based reference measurements are scarce.

Dust reanalyses, utilising state-of-the-art assimilation systems and novel observations for dust assimilation, were also produced for two case studies. These showed the benefits of synergistic observations in the form of profiles and column-integrated quantities. An analysis using Infrared Atmospheric Sounding Interferometer (IASI) dust optical depth for September 2021 was the main scientific contribution from ECMWF. It showed the benefits of using infrared information for dust aerosols within the Integrated Forecasting System (IFS) in composition configuration. The dust interacts with strong meteorological features, such as hurricanes, and deposition is higher where precipitation occurs. This implies a dependency of the dust aerosol distribution on both transport

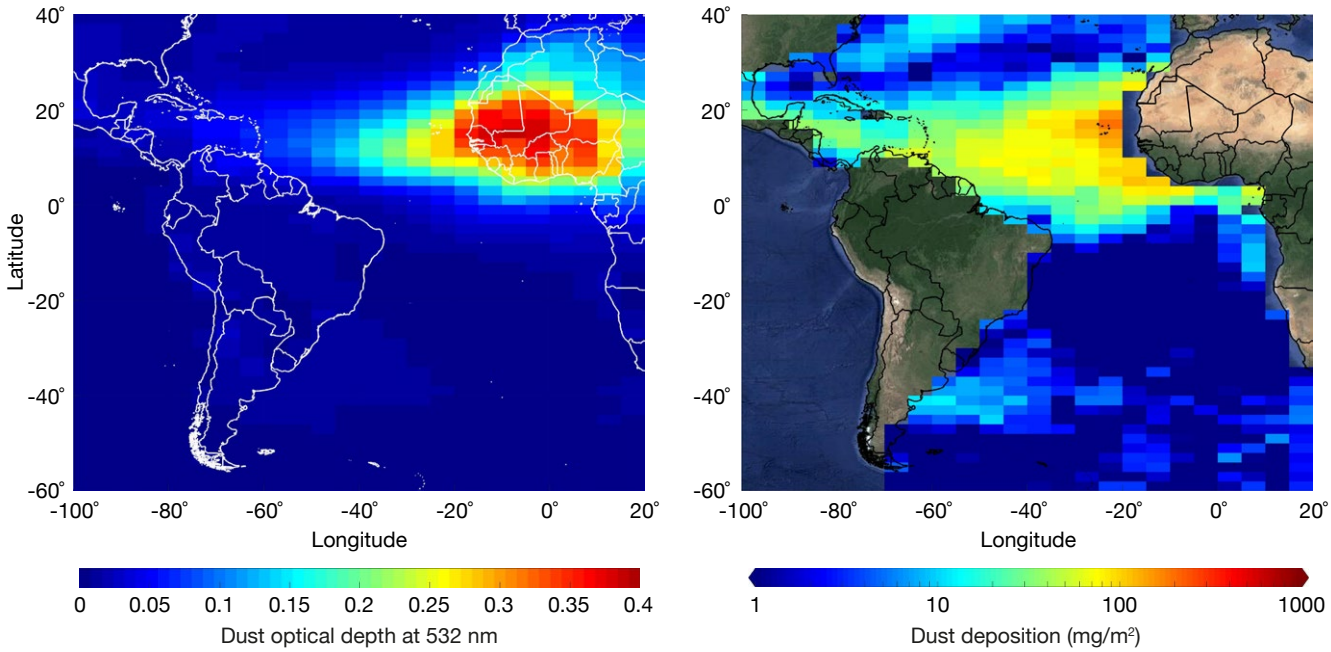

Dust optical depth and dust deposition over the Atlantic. Annual mean dust optical depth at 532 nm (left) and DOMOS dust deposition rate product (right) for the period 2007–2020. Credit: Emmanouil Proestakis (NOA)

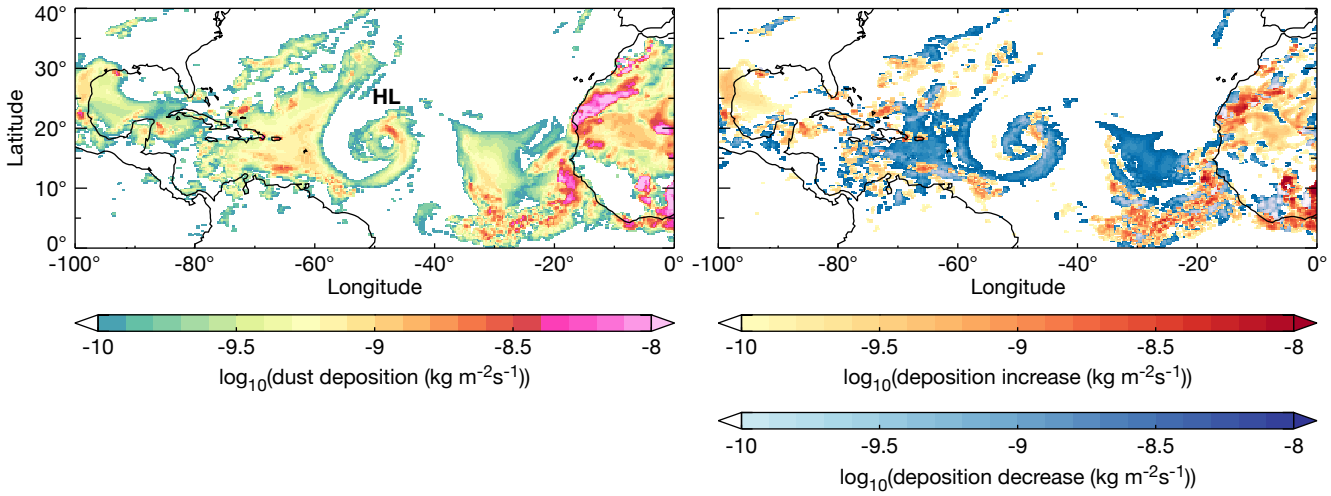

Dust deposition during Hurricane Larry. Dust deposition field from the assimilation of dust aerosol optical depth at 10 micron as measured by IASI/Université libre de Bruxelles (left) and the difference with respect to an IFS-composition control run on 5 September 2021. Hurricane Larry is labelled 'HL'. Credit: Liam Steele (ECMWF)

and precipitation processes. There could also be an impact of dust aerosols on precipitation through radiative processes in pre-hurricane conditions (see the example plots for Hurricane Larry).

Model reconstructions of dust and iron deposition from the EC-Earth3-Iron model were also produced by BSC for the period 1991–2020. An evaluation and comparison with the DOMOS-LIVAS dataset, using the Aeroval platform (https://aeroval.met.no/) developed by MetNo, was also performed for dust optical depths and dust deposition fields. This was done using the EC-Earth3 model run as well as the Copernicus Atmosphere Monitoring Service (CAMS) reanalysis, showing strengths and weaknesses of the models in reproducing the seasonality of dust fields.

More dust and iron but not phytoplankton

The EC-Earth3-Iron datasets enabled the study of the ocean response to changes in iron sources. Dust remains the most important iron source, with fossil fuel becoming more important over the years, particularly in winter, as well as biomass burning. The use of new dust and iron deposition datasets in an ocean biogeochemistry model showed that the phytoplankton primary production is not increased where the deposition is higher, contrary to what was expected. However, there is an overall increase in iron storage within the ocean, which could affect the seasonality of the phytoplankton primary production and therefore modify the climate feedback from the ocean.

Written on behalf of the ESA DOMOS project consortium, Contract Nr. 4000135024/21/I-NB.

An artistic view of ECMWF wave forecasts

Jean Bidlot

On 30 October 2023, Jean Bidlot represented ECMWF at the inauguration of the new artwork 'HavObservatoriet' in Vejle, Denmark. The structure was designed by the internationally recognised artists Lise Autogena and Joshua Portway. The software behind the piece downloads the latest ocean wave forecast from ECMWF several times a day and transforms it to create a visual representation of current wave conditions in the seas surrounding Denmark.

HavObservatoriet is a circular steel edifice, three metres high and seven metres in diameter, which was installed in the Vejle Klimaparken, not far from the famous building complex Bølgen 'The Wave' (see the photo). A purpose-built circular LED screen surrounds the viewer with a visualisation of the current sea state at changing positions in the seas around Denmark.

Lise and Joshua have explored new ways of interpreting and visualising the dynamic movements of the sea in collaboration with ECMWF. The software developed by the artists converts the spectral wave information in the forecasts into a three-dimensional animation of the sea state by processing the forecast data to create a higher-resolution spectral map. Using that map, the artists have created an animated visualisation of the waves as represented by millions of moving floating points that surround the viewer. In this way, they have achieved a realistic representation of what would be seen if one were drifting with the waves at that location (see the wave image).

The sea observatory is the first of a series of works of art in the Vejle Ådal and Fjord region as part of the project 'Byen, Vandet og Kunsten' (City, Water and Art). It was commissioned by the Danish Arts Foundation and focuses on water as a future challenge and potential. The sea observatory is part of the area renewal programme in Vejle Municipality and is supported by the regional renewal funds of the Danish Social and Housing Authority. HavObservatoriet was also supported by ECMWF and the Art, Design and Media Research Centre (ADMRC) at Sheffield Hallam University, UK.

Artwork in Denmark. The HavObservatoriet in Velje Klimaparken with the building complex 'The Wave' in the background.

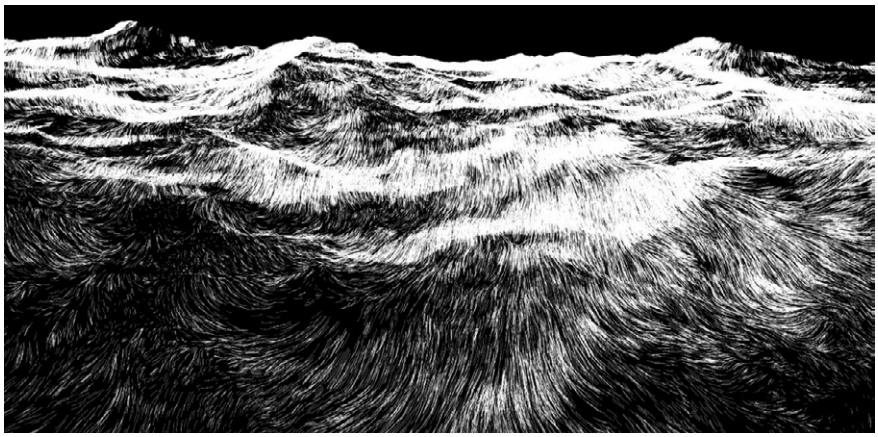

Wave image. Tracing points following the reconstructed wavy surface. More images can be seen on the HavObservatoriet website: https://www.havobservatoriet.net/.

New observations October – December 2023

The following new observations were activated in the operational ECMWF assimilation systems during October – December 2023.

Observations	Main impact	Activation date
MODE-S aircraft observations (re-activation following revision to thinning)	Temperature and wind in the troposphere over Europe	21 November 2023

Optical turbulence forecasts using ECMWF products support Large Binocular Telescope

Elena Masciadri (INAF – Arcetri Astrophysical Observatory)

ECMWF products help the ALTA Center in Italy to forecast optical turbulence in order to support astronomical ground-based observations of the Large Binocular Telescope (LBT) in Arizona, USA.

The impact of turbulence

Turbulence in the Earth's atmosphere strongly limits the resolution of ground-based astronomy in visible and infrared wavelengths. Resolution measures the ability to detect the smallest details of images taken in the focal point of an optical system. Telescope resolution is, in theory, inversely proportional to telescope diameter size: the larger the telescope diameter, the higher the resolution. In reality, because of the presence of atmospheric turbulence, ground-based top-class telescopes (8–10 m in diameter) cannot achieve their potential intrinsic resolution unaided. Such turbulence is called 'optical turbulence'. It is triggered by fluctuations in temperature that determine fluctuations in the refractive index of the atmosphere. This in turn influences the amplitude and phase of wavefronts that interact with the atmosphere. When light wavefronts pass through the atmosphere, they are not any more perfectly plane, as they are when they travel in empty space. Consequently, observed point sources (for example stars) are revealed on the ground-based telescope detector as spots in which the light intensity is spread over a set of large, blurred surfaces instead of being concentrated in individual points.

Adaptive Optics (AO) techniques exist today to correct wavefront perturbations induced by optical turbulence, but AO performance strongly depends on turbulence conditions. It is therefore mandatory to know turbulence conditions in advance to optimise the use of telescopes. It is indeed known, for example, that the most challenging scientific programmes frequently require the weakest turbulence conditions. When turbulence conditions are less favourable, it might be more efficient to perform scientific astronomical programmes that do not require the best resolution. Knowing turbulence conditions in advance thus leads to an efficient use of these complex facilities. This is important to achieve the most relevant progress in our knowledge of the universe. The cost of a night of observation for a telescope of the present generation is in the order of one hundred thousand dollars. It is therefore crucial to optimise the exploitation of these facilities, and in particular to allocate observation time for scientific projects in the presence of suitable turbulence conditions that can guarantee the best outputs.

The role of ECMWF's forecasts

The ALTA Center (alta.arcetri.inaf.it and https://www.lbto.org/weather-forecast/) is an automatic forecasting system that was conceived and developed in 2015 to provide nightly forecasts of optical turbulence and atmospheric parameters relevant for ground-based astronomy to support the science operations of the LBT (see the two photos). The forecasting system is based on a mesoscale model (Meso-NH – mesoscale-non-hydrostatic, developed by the CNRM-Météo-France/Laboratoire d'Aerologie, Toulouse, France) and code expressly conceived for optical turbulence (Astro-Meso-NH, see Masciadri et al., 1999, *A&AS*, **137**, 185). Since 2016, the ALTA Center

Large Binocular Telescope. The Large Binocular Telescope (LBT) located at Mt. Graham (Arizona, US) (left), and an internal view in which two mirrors of 8.4 m in diameter are visible (right - copyright: Wiphu Rujopakarn/Marc-André Besel).

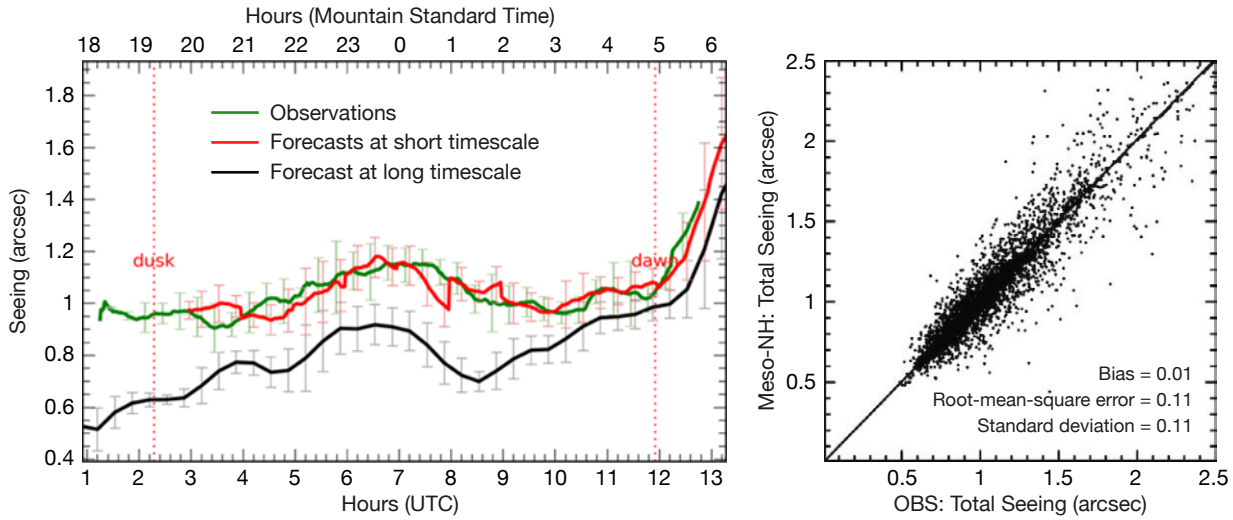

Temporal evolution of seeing and model performance. The left-hand plot shows the temporal evolution of seeing during the night of 10 October 2020 at the LBT. The red line shows forecasts at a short timescale (1 h), the black line shows a forecast calculated at the beginning of the afternoon for the coming night, and the green line shows observations. The smaller the y-axis values, the lower is the optical turbulence level in the atmosphere. The right-hand plot shows optical turbulence forecast performances on a time scale of 1 h calculated over 1 solar year (Masciadri et al., 2020, *MNRAS*, **492**, 140).

has been supporting astronomical observations at the LBT. To set up the ALTA Center, the Astro-Meso-NH package has been transformed into an automatic forecasting system that is fed with initialisation and forcing data coming from ECMWF. Starting from the optical turbulence vertical distribution over the whole atmosphere, a set of further astroclimatic parameters, such as the wavefront coherence time, the isoplanatic angle and the ground layer fraction, which are useful to characterise AO performance, are retrieved, too. The ALTA Center provides forecasts at long time scales (in the afternoon for the coming night) and at short time scales (time scales of few hours, typically one or two hours). The latter are the most critical for the 'flexible scheduling' of observations, i.e. the scheduling of observational programmes depending on turbulence conditions. The first plot in the second figure shows the temporal evolution of 'astronomical seeing', which is a measure of the degradation of the image of an astronomical object due to turbulence in the atmosphere. It shows forecasts on short timescales and on a long timescale as well as observations. The second plot shows ALTA Center performances in forecasting the optical turbulence on a timescale of one hour calculated on a sample of one solar year.

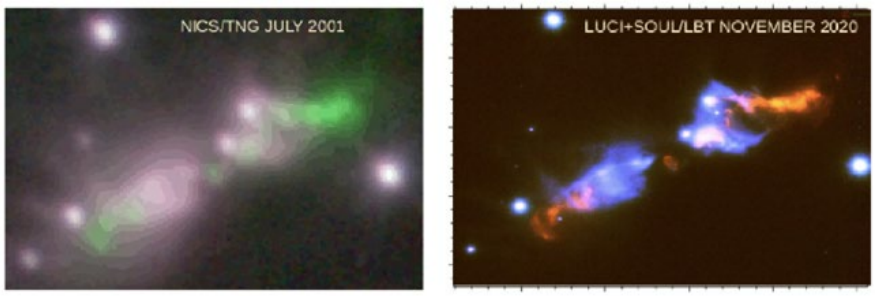

The benefits of SOUL. Image of a massive young stellar object (IRAS 20126+4104) and its outflow obtained without AO (left) and with the AO system SOUL of the LBT (right). Different colours indicate different bands. (The right-hand image is from Massi et al., 2023, *Astronomy & Astrophysics*, **672**, A113, https://creativecommons.org/licenses/by/4.0/.)

A new Adaptive Optics system

The LBT is made up of two 8.4-metre telescopes mounted on the same structure. When it works in interferometric mode, its diameter reaches the equivalent value of 22.4, delivering the sharpest images ever obtained in the visible and infrared regimes by a single telescope. The LBT can therefore be considered the precursor of the new generation of Extremely Large Telescopes (ELTs) (30–40 m) and, at present, is the ground-based telescope with the largest equivalent diameter size in the world. The ALTA Center supports science operations of observations performed with present, forthcoming, and future astronomical instruments of LBT. In recent years, the LBT Observatory has invested in a new AO system called SOUL (Pinna et al., 2021, DOI:10.48550/arXiv.2101.07091). This makes it possible to strongly improve image resolution and to discern many more point sources that would not be visible otherwise. It also means we can go deeper into the Universe. The last figure shows the image of a massive young stellar object with its outflow as observed without any AO system and with the AO system SOUL. New high-contrast imaging instruments (SHARK-NIR and SHARK-VIS), using SOUL, will see the light in the forthcoming two years. Using initialisation and forcing data from ECMWF, the ALTA Center will be able to play a crucial role in identifying the best atmospheric conditions to carry out the most challenging astrophysical observations.

New group formed to protect spectrum for meteorology and Earth observation

Stephen English

In an initiative led by the European Space Agency (ESA), three European organisations – ECMWF, ESA and EUMETSAT (European Organisation for the Exploitation of Meteorological Satellites) – and representatives from the European Earth observation, weather and climate science communities have come together to form a new group, ESSEO (European Scientists on Spectrum for Earth Observation), to respond to ever growing concern over Radio Frequency Interference (RFI). This kind of interference affects science services now and is expected to do so even more in the future. Here Stephen English describes the background and the activities of ESSEO, which is chaired by ECMWF.

Sharing of the radio spectrum

In the summer of 2019, an ECMWF Newsletter article provided a viewpoint on the threat and opportunity for meteorology at the World Radiocommunication Conference (WRC) 2019 (*https://www.ecmwf.int/en/newsletter/160/viewpoint/why-we-need-protect-weather-prediction-radio-frequency-interference*). The WRC is the forum that updates the international Radio Regulations, and it is held approximately every four years. These regulations determine the agreed rules under which radio signals can be transmitted. This is of critical importance to the integrity of the global observing system for weather and climate and other Earth observation activities.

As was noted in the 2019 article, a range of global forecast metrics (such as Forecast Sensitivity to Observation Impact, FSOI) show that typically around a third to half of weather forecast error reduction from observations comes from satellite observations that rely on regulatory protection of key spectral bands. This applies both to global numerical weather prediction (NWP) (Bormann et al., 2018) and, mainly via lateral boundary conditions, regional NWP (Randriamampianina et al., 2021). In particular, this is critical for some of the observations which have the highest impact on the skill of NWP, such as microwave temperature and humidity sounders. Up to now, recorded cases of radio frequency interference are mostly below 20 GHz, making it particularly a concern for the Copernicus Imaging Microwave Radiometer, which will be a Sentinel mission under the Copernicus Expansion Missions programme. Other observations also rely on protection, e.g. for downlinks from satellites (there are cases of disruption to the GOES data downlink, for example) and communication of in-situ observations (e.g. radiosondes that use 400–406 MHz transmissions). The radio spectrum, which here can be considered to be frequencies from 1 kHz to 1 THz, is used in many applications. Many of these are expanding, including applications in the fields of weather and climate and other Earth observation activities. The requirements for new generations of mobile phone communications also involve ever increasing swathes of bandwidth. It is important that sharing of the radio spectrum, a unique and valuable resource, is done fairly, taking into account the requirements of diverse application areas.

From WRC-19 to WRC-23

In 2019, the focus was very much on one particular meteorological band: 24 GHz. There had been much controversy in the media concerning a potential threat to this band from 5G. The discussion at WRC-19 was critical to the long-term protection of this band. The outcome from WRC-19 fell short of the position published by the World Meteorological Organization (WMO) in its position paper for WRC-19 (WMO, 2019). However, at least some protection was afforded, and after WRC-19 further discussions were held, notably in Europe, that further improved the situation regionally for 24 GHz. It should be noted that the WMO had 12 agenda items of concern for meteorology, and achieved satisfactory outcomes in 11.

Now, four years on, attention turned to WRC-23. Again there were a number of concerns and opportunities, and once again the WMO published a position paper (WMO, 2023), to inform its negotiating position. Once again, the WMO's team was highly successful, due to the diligence and hard work at the WMO and by spectrum managers from various institutes. Progress was even made in a difficult area concerning C-band. The 5G community was seeking additional spectrum in the 6.425–7.125 GHz band, which overlaps with the bands used by passive sensors near 6.9 GHz. Examples are the AMSR-2 instrument on the Japanese GCOM-W satellite and the future CIMR (Copernicus

doi: 10.21957/se6va51pt3

Imaging Microwave Radiometer) mission, part of the Copernicus Expansion programme, which is currently under development by ESA. The 6.9 GHz band is the only source of sea-surface temperature information in persistently cloudy areas, such as underneath a tropical storm that could develop into a damaging hurricane or typhoon. Unfortunately, although this band has been used since the 1970s (it was part of the SMMR channel set first launched in 1978; see *https://space.oscar.wmo.int/instruments/view/smmr*), it has never been afforded protection in the Radio Regulations. The Radio Regulations merely acknowledge its use for ocean measurement without explicitly protecting it: the exact text says that "administrations should bear in mind" the use of this band by Earth observation (EO) sensors. Studies at ANFR (Agence National des Fréquences, France) have predicted that RFI from land-based 5G installations will affect observations 2,000 km out to sea. This could significantly impact weather forecasts, notably for extreme events, such as tropical cyclones.

In addition to this major issue at 6.9 GHz, there were also important discussions concerning a range of microwave frequencies (10.65 GHz, 18.7 GHz and 36.5 GHz, which are important for liquid cloud and terrestrial surface information; and 243 GHz). The lower frequency channels are particularly relevant for the forthcoming Copernicus Imaging Microwave Radiometer.

The need for ESSEO

It is recognised that the science community needs to do more to communicate the importance of all bands used for weather and climate: why they are important, how they are used, and what their impact is. This needs to include passive observations (where we measure natural emissions from the Earth and the atmosphere) and active observations (where we use radar to infer surface or atmospheric information). In the United States, the Committee on Radio Frequencies (CORF) works under the auspices of the National Academies of Science to give a wide-ranging scientific perspective on the value of bands. Until recently, there was no equivalent in Europe. Space agencies (ESA, EUMETSAT) and EUMETNET spectrum managers provided expert contributions to the International Telecommunication Union (ITU), and the WMO and some national meteorological and hydrological services (such as the UK Met Office or Météo-France) have dedicated spectrum managers, who also participate in this process. However, there was no mechanism to ensure review by the wider scientific community of the science case, to ensure it is correct, robust and defendable. Therefore, ESA took the initiative to set up a new group: European Scientists on Spectrum for Earth Observation (ESSEO). From the outset, this has been a collaborative effort between ESA, EUMETSAT and ECMWF. The group is chaired by Stephen English with strong support from ESA and EUMETSAT spectrum managers. It also includes a group of leading scientists from a number of research facilities across Europe, bringing expertise in the understanding and use of passive and active radio spectrum observations. It is narrower in focus than CORF, but gives a voice to science for Earth observations.

Given the timeline, the main focus of ESSEO is towards WRC-27, in about four years' time. However, WRC-23 was critical for ESSEO's work plan because it finalised the agenda items for WRC-27. The way WRC works is to consider proposals for the agenda for the next meeting, in four years' time, at the end of the current meeting, and to then set that agenda. This gives all stakeholders a chance to do the studies needed to establish if there is a concern or not in their application area ahead of the next meeting. Therefore, the work of ESSEO towards WRC-27 really began in earnest with the publication of the WRC-27 agenda. However, there was already a published preliminary agenda for WRC-27 before WRC-23, so ESSEO already had a good idea of the items that might be retained, and it had been doing preliminary work during 2023. Unusually, it is not just meteorology defending its existing bands, but proactively seeking a permanent and properly protected home for C-band marine observation.

The ESSEO team comprises Stephen English (Chair, ECMWF), Catherine Prigent (CNRS, France), Alessandro Battaglia (PoliTo, Italy), Andrea Monti-Guarnieri (PoliMi, Italy), Chawn Harlow (Met Office, UK), Guilia Panegrossi (CNR, Italy), Jesse Andries (WMO), Ken Holmlund (retired, Finland), Markus Dreis (EUMETSAT), Patrick Eriksson (Chalmers University, Sweden), Philippe Chambon (Météo-France), and Yann Kerr (CESBIO, France). They have worked closely with the ESA team, which is made up of Yan Soldo, Bruno Espinosa, Flavio Jorge, and Josep Rosello.

Issues for WRC-27

WRC-27 seems likely to be a very important WRC for weather and climate science, as the Agenda Items (AIs) listed in Table 1 have a potential impact on Earth observations.

In view of the concerns discussed earlier about the future of C-band for passive sensing, the potential for new allocations in C-band for sea-surface temperature (SST) close to 4 and 8 GHz is positive. The concept would be for a future radiometer to operate at the same time at 6.9 GHz, for long-term continuity in RFI-free areas, and in the new bands, to provide SSTs in areas where there is RFI concern at 6.9 GHz. As both new channels would be available in RFI-free

AI	Topic	Earth Exploration Satellite Service bands
1.1	GSO (geostationary satellite orbit) ESIM (Earth stations in motion) in 37.5–51.4 GHz	36–37 GHz, 50.2–50.4 GHz
1.7	6G in 7–24 and 92–275 GHz	Several passive and active bands
1.8	Radars above 230 GHz	226–231.5 GHz, 235–238 GHz, 239.2–242.2 GHz, 244.2–247.2 GHz, several bands above 275 GHz
1.11	Space-to-space MSS (mobile satellite services) in 1.5–2.5 GHz	1215–1300 MHz 1400–1427 MHz 1525–1535 MHz
1.14	Narrowband MSS in 1.7–3.4 GHz	1.4–1.427 GHz, 2.64–2.7 GHz, 4.2–4.4 GHz 3.1–3.3 GHz 1.525–1.535 GHz
1.17	Space weather sensors	Several passive and active bands
1.18	Protection of RR (Radio Regulations) 5.340 bands > 86 GHz	86–92 GHz, 114.25–116 GHz, 148.5–151.5 GHz, 164–167 GHz, 182–185 GHz, 190–191.8 GHz, 200–209 GHz, 226–231.5 GHz
1.19	New EO (Earth observation) band (mostly for SST (sea-surface temperature)) in 4–10 GHz	4.2–4.4 GHz, 4.95–4.99 GHz, 6.425–7.25 GHz, 8.4–8.5 GHz (last band not allocated)
2.10	EO uplinks in 22.55–23.15 GHz	22.21–22.5 GHz, 23.6–24.0 GHz

TABLE 1 Topics for the WRC-27 agenda.

areas, it would be straightforward to intercalibrate between SSTs using 6.9 GHz and SSTs using the new bands. Also of interest is the consideration of bands above 275 GHz, which will be considered for the first time. This is important for the new Ice Cloud Imager on the EUMETSAT Polar System – Second Generation (EPS-SG), and for the radiometer that will fly on the EPS-Sterna constellation, which will follow ESA's Arctic Weather Satellite Proto Flight Model (AWS PFM).

There is concern over the future status of bands currently fully protected by footnote 5.340 of the Radio Regulations above 86 GHz. This includes the water vapour band at 183 GHz, which – according to the Forecast Sensitivity Impact Observation metric – contributes most to forecast error reduction at ECMWF. There are new concerns close to 24 GHz, and further concerns in L-band close to the channel used by Soil Moisture and Ocean Salinity (SMOS), Soil Moisture Active Passive (SMAP) and Copernicus Imaging Microwave Radiometer (CIMR) instruments. There are also concerns for the window channel for the temperature sounding band (50 GHz) and the cloud liquid water and surface snow pack band (36.5 GHz). Finally, 6G mobile networks are expected to seek additional spectrum in the 7–30 GHz range, but the exact frequencies are not clear yet. ESSEO is assembling information on the use of all these bands in different application areas. This will lead to a science report available early in 2024, which will both inform and guide spectrum management discussions. It would be of great help if the wider European science community could provide input to the ESSEO Chair or Yan Soldo to ensure this paper is as broad and as accurate as possible.

ESSEO assessment of existing RFI

As well as providing a trusted and consensus science input on WRC issues, the ESSEO group will also monitor the status of RFI and help with the process of reporting. RFI affects sensors in the Earth Exploration Satellite Service (EESS) in many ways. On rare occasions, RFI will be large and easily spotted. Very strong RFI may damage the satellite receiver, in which case the loss of science data would be permanent. More typically, and often of greater concern, is when the level of RFI is small and indistinguishable from real natural variability. However, as this natural variability is the signal for weather and climate, small RFI will lead to unknown errors in the analysis, and therefore errors in prediction and climate monitoring. If there is even a possibility of this, the only safe option is to stop using the observations, because using them is liable to make the analysis worse.

Even if technology- or software-based mitigation of RFI is possible, RFI has an impact in terms of the cost of designing and operating instruments. For example, modifications would be required to better cope with the RFI environment and, during operations, to process measurements for RFI. Whilst some cases of RFI can be detected and data can be either rejected or corrected, not all RFI can be managed by software or hardware improvements. Therefore, regulatory

protection through the WRC is essential, and RFI reporting is of critical importance. However, this implies additional cost and effort for space agencies and for users of these observations.

At the present time, it is known that many EESS sensors are affected by RFI (Draper 2018; SFCG 2023). However, few have taken steps towards reporting the presence of RFI to the proper national regulatory authorities or to the ITU, and it is known that the issue of RFI to EESS sensors is largely under-reported. This is in part due to the challenge of unambiguously identifying RFI, but also because these instruments have a spatial resolution of tens of kilometers, which is too large for practical actions to be taken to pinpoint the source. In recent years, however, algorithms have been developed to locate RFI sources with accuracies much finer than the size of the footprint, typically within a few kilometers. Such accuracy has proven precise enough for national regulatory authorities to identify the RFI sources reported by EESS sensors (e.g. at L-band for SMOS). ECMWF's long-term monitoring of the observation-minus-background differences for SMOS has shown how over the years many RFI sources have been identified and shut down.

Conclusions

The radio frequency spectrum is a valuable and unique resource supporting many critical application areas, including amongst others mobile communications, Earth observation, weather forecasting, climate monitoring, radio astronomy, command and control for satellites, and data downloads from satellites. All have genuine requirements and bring real socio-economic benefits, but at times these requirements will come into conflict. The WRC is the key international forum to resolve these areas of potential conflict, and it is vital that the WRC has the best possible information. To ensure this, those representing weather and climate science and Earth observation in general should have watertight science to back up the position taken on our behalf by the WMO. This is the purpose of ESSEO. RFI contamination is likely to become worse over time, as many terrestrial and spaceborne services plan to rely more heavily on the spectrum. Therefore, this collaboration between ECMWF and space agencies, through ESSEO and also more generally, will become ever more important to weather and climate services.

Further reading

WMO, 2019: WMO POSITION ON WRC-19 AGENDA, WRC-19-IRWSP-19/3-E.

WMO, 2023: WMO Position on the World Radiocommunication Conference 2023 (WRC-23) Agenda. Cg-19/Doc. 4.2(10).

Draper, **D.W.**, 2018. Radio frequency environment for Earth-observing passive microwave imagers. *IEEE Journal of Selected Topics in Applied Earth Observations and Remote Sensing*, **11(6)**, 1913–1922.

SFCG, 2023: Space Frequency Coordination Group (SFCG), RFI to EESS Sensors, *https://www.sfcgonline.org/RFI to EESS Sensors/default.aspx*, accessed on 5 July 2023.

Bormann, **N.**, **H. Lawrence**, & **J. Farnan**, 2019: Global observing system experiments in the ECMWF assimilation system. *ECMWF Technical Memorandum* **No. 839**. *https://doi.org/10.21957/sr184iyz*

Randriamampianina, **R.**, **N. Bormann**, **M.A.Ø. Køltzow**, **H. Lawrence**, **I. Sandu** & **Z. Wang**, 2021: Relative impact of observations on a regional Arctic numerical weather prediction system. *Q. J. R. Meteorol. Soc.*, **147**, 2212–2232. *https://doi.org/10.1002/qj.4018*

Improved two-metre temperature forecasts in the 2024 upgrade

Bruce Ingleby, Gabriele Arduini, Gianpaolo Balsamo, Souhail Boussetta, Kenta Ochi (Japan Meteorological Agency), Ewan Pinnington, Patricia de Rosnay

Two-metre temperature (T2m) is a key forecast variable. Here we describe how changes to ECMWF's Integrated Forecasting System (IFS), which are expected to become operational as part of IFS Cycle 49r1 in 2024, improve short-range forecasts of T2m. Physics changes in IFS Cycle 49r1 will include extensive improvements to surface vegetation fields and changes to make the interpolation of the temperature to 2 m more realistic. There have also been major upgrades to the data assimilation system, which establishes the initial conditions of forecasts (the 'analysis'). Currently, T2m ('screen temperature') and two-metre humidity ('screen humidity') from SYNOP weather station reports and METAR aviation weather reports are assimilated in a separate land surface analysis – primarily to update initial soil moisture and temperature conditions. However, only daytime screen humidity is assimilated in the atmospheric component of the data assimilation system, 4D-Var. In IFS Cycle 49r1, T2m will be assimilated in 4D-Var. This proved beneficial after extensive testing/tuning. Improvements in the separate snow data assimilation system as well as in T2m and soil moisture land data assimilation are also applied. Overall this results in better T2m forecasts, especially in northern hemisphere winter.

New vegetation maps and soil moisture stress representation

The new land-use and land-cover (LULC) maps of the European Space Agency (ESA) Climate Change Initiative and the new Copernicus Global Land Services-based leaf area index (LAI) maps have been successfully tested and included in Cycle 49r1. As well as using the new maps, several model changes were made towards a more realistic physical representation. The first change is the implementation of a new LAI observation operator, which enables a conservative disaggregation of the observed LAI into high and low vegetation components. This resulted in a more accurate seasonal variability of vegetation. The second step is the implementation of a more realistic soil moisture stress function. The updated stress function mimics the behaviour of the soil matric potential, a measure of the relative availability of water in the soil for plant uptake, and allows plant roots to better extract water, especially in relatively dry conditions. The third change affects mainly winter and spring seasons by explicitly allocating the surface albedo for forests with snow underneath from processed satellite data rather than relying on tabulated values.

With these changes, the near-surface atmospheric variables still needed additional adjustment for acceptable NWP skill. Model parameters were first optimised for individual grid points based on in-situ observations (FLUXNET) and in surface standalone mode. This enabled a better match of the surface fluxes with in-situ observations. The second level of model parameter adjustments uses global offline surface simulations for which the near-surface parameter errors are stratified by vegetation type. The minimum stomatal resistance (a plant characteristic that represents the degree of opposition of the plant leaf to release water vapour to the atmosphere) is used to adjust T2m and relative humidity, mainly for spring and summer. In Figure 1, the improvements brought by the land-use and land-cover package and associated model changes are illustrated for temperature cross-sections for different latitudes and pressure levels at several forecast ranges.

Modified 2-metre temperature diagnostic formula

Two-metre temperature is a diagnostic variable in the IFS, which means that it is not predicted directly by the model but is derived from other variables. This involves a vertical interpolation between surface (skin) temperature and the lowest model level temperature using Monin-Obukhov similarity theory. To avoid possible runaway cooling, the interpolation function used in Cycle 48r1 and earlier was tapered to the lowest model level temperature for relatively high stability (see Figure 2a). In Cycle 49r1, a modified interpolation function is introduced that is closer to the theory and smoother, avoiding the abrupt jump to the lowest model level temperature at a fixed value of stability.

The introduction of the revised diagnostic formula shows a significant improvement in root-mean-square (RMS) error in the northern hemisphere at short lead times (see Figure 2b), due to a more realistic evolution of T2m in stably stratified conditions.

doi: 10.21957/bi49s20qa8

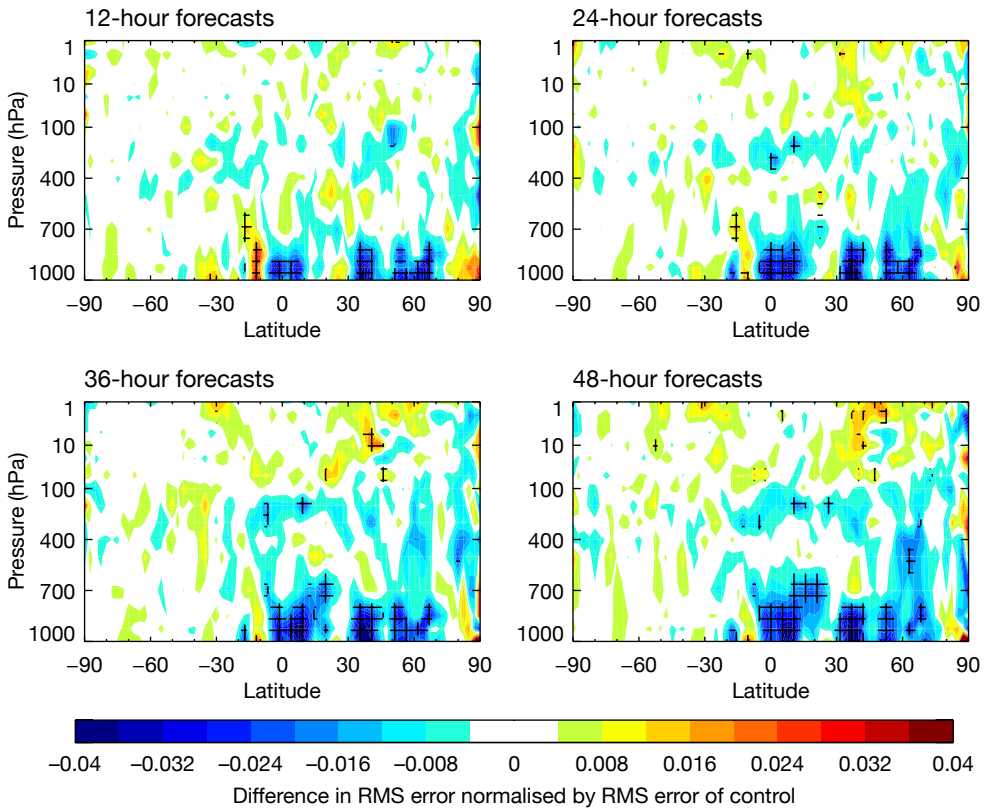

FIGURE 1 Temperature forecast improvements related to the vegetation changes and associated modifications are shown in the blue areas, which correspond to a reduction in the root-mean-square (RMS) error of the temperature forecasts. The tests were carried out from 5 June 2020 to 31 August 2020. Forecasts were verified against each experiment's own analysis, and cross-hatching indicates statistical significance at the 95% confidence level.

Atmospheric assimilation of 2-metre temperature and other surface variables

For many years, assimilation of SYNOP temperature and humidity data was standard in limited-area models, but not in global systems. In 2008, the UK Met Office global model started to assimilate these data, and in 2022 the German weather service (DWD) followed suit.

At ECMWF, tests assimilating T2m in 4D-Var gave large improvements in short-range T2m forecasts, but in some winter regions 850 hPa temperatures were degraded, partly due to unrealistic coupling in stable conditions. Remedies aimed at retaining the T2m benefits, while reducing the problems, were explored.

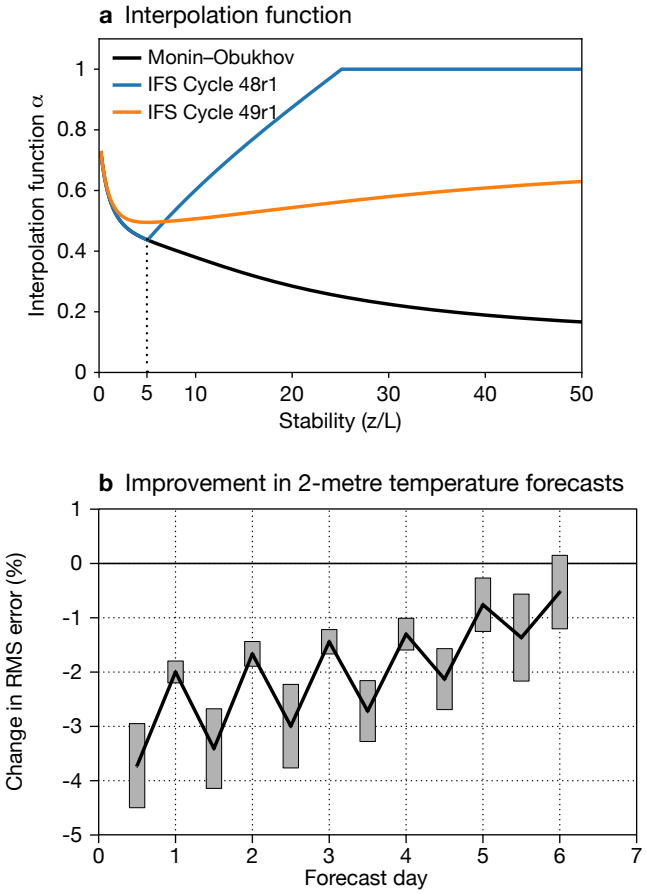

FIGURE 2 We show (a) the interpolation function, α, as a function of stability, which is defined as height above ground/Obukhov length (z/L). α=1 indicates that T2m equals T at the lowest model level; α=0 indicates that T2m equals the skin temperature. The black line shows the function based on Monin–Obukhov theory, the blue line indicates the current interpolation formula (Cycle 48r1), and the orange line indicates the new function to be introduced in Cycle 49r1. We also show (b) the improvement (negative) in T2m forecasts due to changes in the interpolation function of T2m. This relates to forecasts for December 2021 to February 2022, for the region 20°–90°N. We show the percentage change in root-mean-square (RMS) error, verified against SYNOP observations. The grey rectangles show 95% confidence intervals.

Reducing the weight given to T2m data with very large departures from the short-range forecast used to establish the analysis (the 'background'), and limiting the assimilation of data to the first six hours of the 12-hour 4D-Var window to produce more localised increments, both helped. Temperature differences of more than 7.5 K are not used. Following these modifications, a large benefit is still seen in northern hemisphere winter (Figure 3): a 5% reduction in RMS error for 12-hour forecasts, decreasing with lead-time when verified against SYNOP data. The benefit in summer and in the tropics is smaller, but still useful.

On average, temperature decreases with height in the troposphere – this is known as the lapse rate. To take account of the difference between station height and model height in 4D-Var, an adjustment is calculated from the height difference using a lapse rate of 5.5 K/km and applied to T2m. This fits the data slightly better than 6.5 K/km, which is often used, including in verification. Stations are used between 400 m below and 200 m above the model height. On average, stations are slightly lower than the model height as they are more likely to be in valleys. There is no bias correction applied, because of the complexity of observation–background T2m biases, and in many cases the background biases are larger than observation biases. The verification shown here uses SYNOP stations within 250 m of the model height, and observations more than 15 K from the analysis are rejected. The assimilated screen humidity variable changes from relative humidity to specific humidity, and it will be used both day and night after the change in Cycle 49r1.

Work at the UK Met Office and elsewhere (see Pauley and Ingleby, 2022) suggests that it is difficult to get a positive impact from assimilating 10 m wind over land. SYNOP wind assimilation was tested with the other changes, but the impact was marginal and the winds will not be assimilated at ECMWF for now. Winds from ships and moored buoys continue to be assimilated. Surface pressure remains the most important surface variable for global NWP.

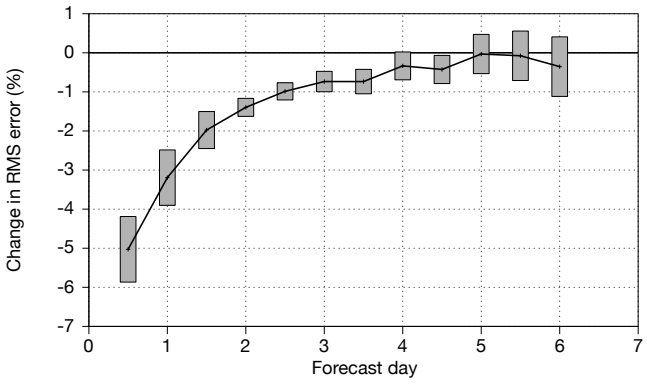

FIGURE 3 The improvement (negative) in T2m forecasts due to 4D-Var assimilation of T2m. The plot shows results for the period of December 2021 to February 2022, for the region 20°–90°N. We show the percentage change in root-mean-square (RMS) error, verified against SYNOP observations. The grey rectangles show 95% confidence intervals.

The background errors used in 4D-Var are derived using the ensemble of data assimilations (EDA). In common with other ensemble systems, the EDA has long been underspread near the surface (especially over snow). There is a change to the stochastic physics in Cycle 49r1 that partially addresses this, but as shown in Figure 4, the background error estimate still appears too small in the lowest levels. Larger spread near the surface would tend to increase the size of analysis increments from T2m assimilation at the lowest model level and to reduce them a few levels up, which would be more realistic for winter cases.

Snow data assimilation and improved snow cover

Several major developments were made to improve the snow analysis. This uses both synoptic snow depth reports and the US National Oceanic and Atmospheric Administration's National Environment Satellite, Data, and Information Service (NESDIS) Interactive Multi-sensor Snow and Ice Mapping System (IMS). The use of IMS data has been revised, enabling the exploitation of satellite-based snow cover information in mountainous areas. It reduces IFS positive biases in snow cover and snow depth, with a strong positive impact on atmospheric forecasts. Other changes include an increase in the maximum allowed snow depth value

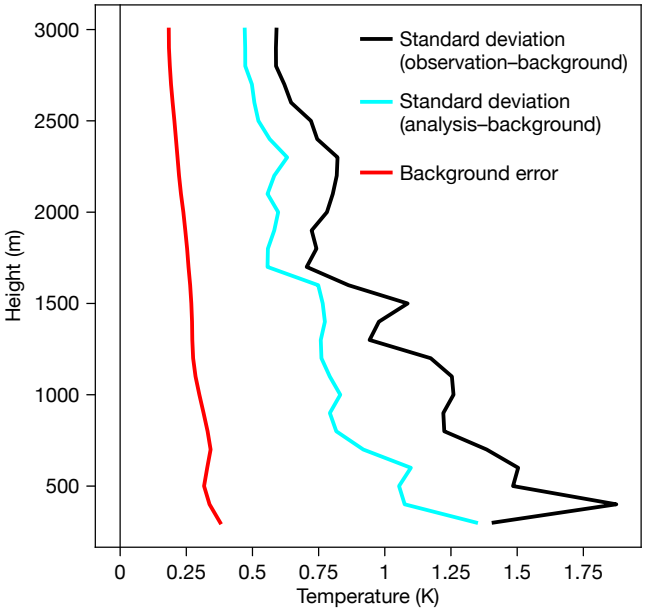

FIGURE 4 Low-level temperature statistics from the radiosonde station at Sodankylä, Finland, for December 2022. The standard deviations of observation-minus-background (O–B) and analysis-minus-background (A–B) are shown, as is the mean estimate of background error based on the EDA.

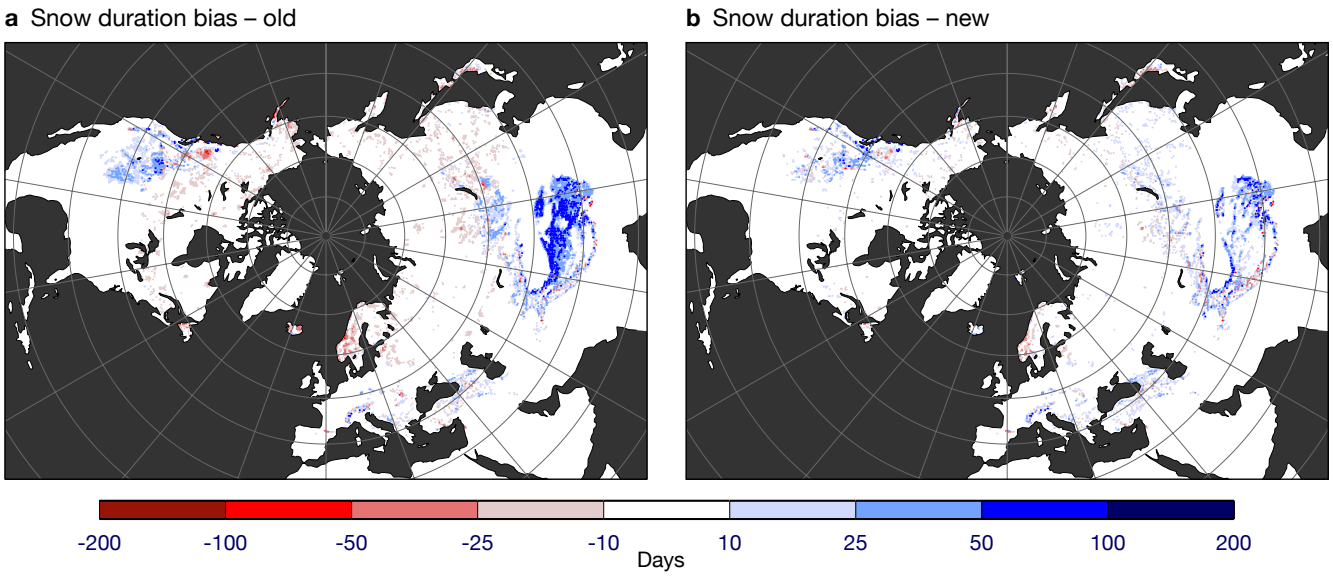

FIGURE 5 Biases of snow duration (number of days when snow depth is more than 1 cm in the model) compared to IMS in March–May 2022 (a) before and (b) after the snow data assimilation changes. Positive biases are reduced in mountainous areas.

from 1.4 m to 3 m in the analysis, and a reduction of the vertical structure function scales from 800 m to 500 m. The latter change increases the weight of observations that have the lowest altitude difference with the model. In addition to data assimilation changes, snow cover parametrization in the snow model was also revised to improve the fraction of ground covered by snow. Both the snow changes were extensively evaluated for winter and summer as well as spring, which is key for snow model and data assimilation (see Figure 5). Other results (not shown) indicate a strong positive impact on T2m, especially in the Rocky Mountains and the Tibetan Plateau areas, with widespread improvements in the troposphere in geopotential hight, vector wind and humidity forecasts in the northern hemisphere in winter.

In the last decade, the World Meteorological Organization (WMO) Snow Watch team has worked to improve the exchange of in-situ snow observations and to assess the quality of satellite snow products. The IFS Cycle 48r1 upgrade, implemented in June 2023, included a change from a single layer snow model to a multi-layer snow model, which makes snow melt more realistic (see Newsletter No. 176: *https://www.ecmwf.int/en/newsletter/176/*).

Soil moisture and 2-metre temperature land assimilation

The soil moisture analysis relies on a Simplified Extended Kalman Filter (SEKF). We assimilate soil moisture products from ASCAT (Advanced Scatterometer) and SMOS (Soil Moisture and Ocean Salinity) satellite instruments along with screen level T2m and relative humidity information. There is a linked 2D Optimal Interpolation analysis of T2m (de Rosnay et al., 2022). These components have been revised, bringing improvements in both winter and summer forecasts, in T2m and near-surface forecasts.
The revisions include the implementation of a lapse rate correction in the T2m analysis to account and correct for altitude differences between the model grid points and the SYNOP observations. An adjustment of 5.5 K/km is introduced, consistent with the lapse rate correction used in the 4D-Var T2m analysis. In the SEKF soil analysis, the background error standard deviation has been doubled, to 0.02 m^3 m^{-3}, giving more weight to the observations used in the SEKF to constrain the soil moisture analysis. Both changes have a substantial positive impact in the tropics and northern hemisphere during summer. Figure 6 shows the effect of these changes, plus the snow changes described above, on the forecast fit to SYNOP temperature in winter: an improvement of about 1% approximately, constant out to day six. The improvement of the forecast fit to our own analysis is larger (not shown).

Combined impact

Figure 7 shows the scorecard against observations for the changes described above. The results are mostly very positive. One of the few exceptions to this is that, in the tropics at 850 hPa, there is a detriment to short-range temperature forecasts. This stems from the interaction of the LULC and T2m assimilation changes: before tuning the assimilation change, the problem was more widespread. The land-surface changes also give slight benefits beyond day 10 (not shown). Figures 8 and 9 show verification of T2m for the whole Cycle 49r1 against SYNOP observations for northern hemisphere winter. Most benefit is seen north of 45°N. Figures 7–9 illustrate the widespread positive impact of the changes

on T2m and atmospheric forecasts. Another change included in Cycle 49r1 is the assimilation of integrated water vapour information from ground-based GPS stations (predominantly over Europe and China for now). This has little impact on T2m forecasts, but it slightly improves short-range screen humidity forecasts. In the northern extratopical winter, the headline result is that Cycle 49r1 improves the 12-hour T2m forecast by more than 9% (Figure 9).

The results presented here all used forecast/analysis grid spacings of 28/80 km. The whole Cycle 49r1 package is now being tested at grid spacings of 9/40 km. The results confirm the previous tests.

Outlook

ECMWF will continue to work on improving T2m forecasts. One aspect is increasing the ensemble spread of near-surface temperatures, especially in winter, as mentioned above. 4D-Var has several outer loops, starting at coarse resolution and then moving to finer scale. We will try putting more weight on the T2m observations in the later outer loops, as the model representation of near-surface temperature improves. Above the boundary layer (i.e. above the part of the atmosphere which is directly influenced by the surface), there is less sensitivity to model resolution. In recent years, partly due to EU policy, some European countries

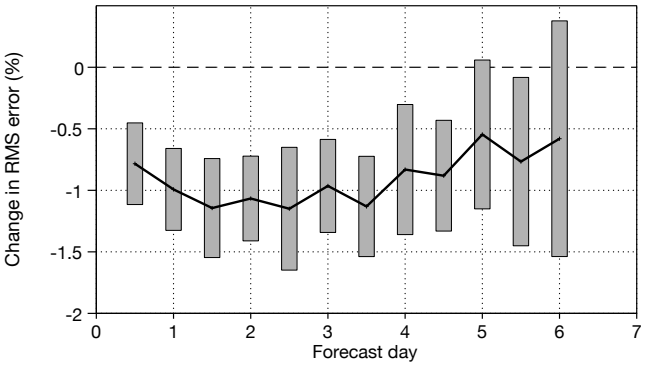

FIGURE 6 Impact of snow, soil moisture and lapse rate changes on verification of predicted temperature against SYNOP temperature 20°–90°N, December 2021 – February 2022. We show the percentage change in root-mean-square (RMS) error. The grey rectangles show 95% confidence intervals.

have started providing data from more stations, and this trend looks set to continue. There is separate work evaluating crowd-sourced observations. In a global NWP system, we are well aware that some parts of the world are sparsely observed. With the WMO and others, efforts to improve data exchange and quality will continue. Also, ongoing developments of coupled land–atmosphere assimilation at ECMWF will enhance the exploitation of surface-sensitive satellite observations and contribute to improving T2m forecasts.

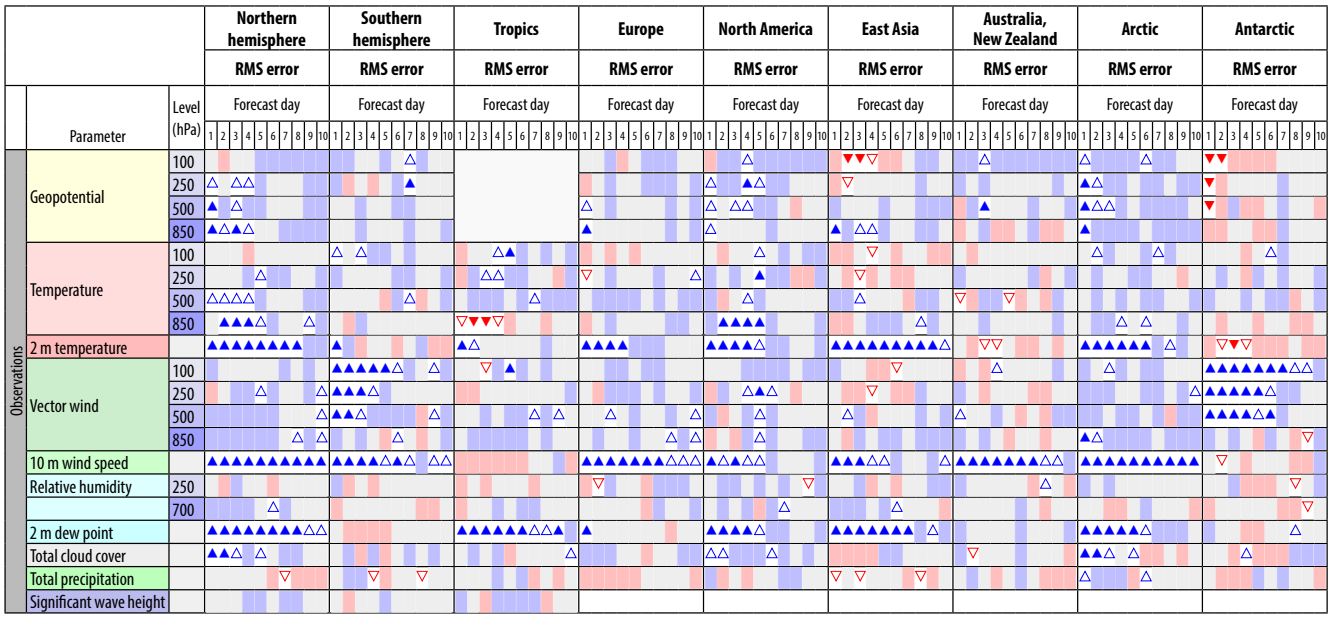

Symbol legend: for a given forecast step...

- ▲ experiment better than control statistically significant with 99.7% confidence
- △ experiment better than control statistically significant with 95% confidence
- experiment better than control statistically significant with 50% confidence
- not really any difference between control and experiment
- experiment worse than control statistically significant with 50% confidence
- ▽ experiment worse than control statistically significant with 95% confidence
- ▼ experiment worse than control statistically significant with 99.7% confidence

FIGURE 7 Scorecard of root-mean-square (RMS) error with respect to observations for winter and summer combined (six months) for the changes described in the text.

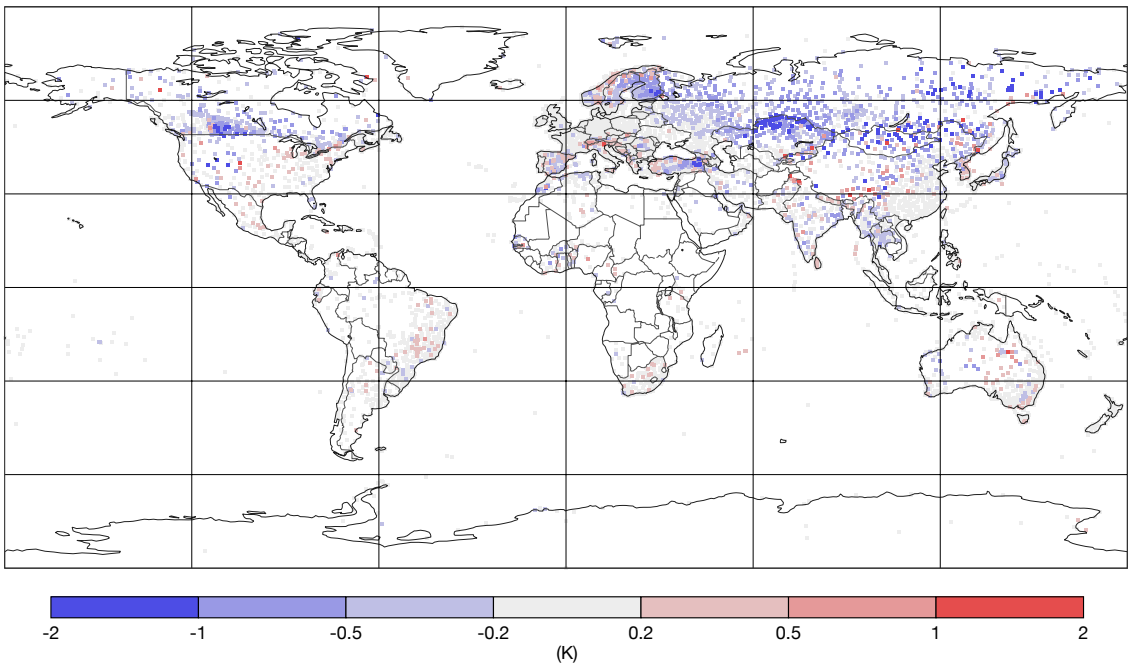

FIGURE 8 Impact on 12-hour verification of T2m against SYNOP observations of the changes to be implemented in Cycle 49r1 from December 2021 to February 2022 at 12 UTC. Blue colours indicate an improvement.

On the land-modelling side, several new developments aim to improve the surface representation and coupling with the atmosphere. These are facilitated by a new climate field generation suite, which enables timely testing of new global vegetation and land input fields; and the prospective Multi-Parameter Regionalisation (MPR) system, which is intended to enable an automated physically-based optimisation of model parameters. Specifically, the T2m forecast would benefit from the improvement of the water, energy and carbon cycles representation. Similar optimisation has already shown benefit for T2m in the DWD system. Future work will also focus on improved vertical soil discretisation and coupling with the hydrological model. It would also benefit from a better representation of snow intercepted by vegetation and improved wind-induced water flux from snow to the atmosphere (sublimation). Over glaciers, a new sub-grid ice representation with a better coupling between snow and ice would also improve the near-surface atmosphere. Finally, anthropogenic impacts are being explored under the very-high-resolution framework of the EU's Destination Earth (DestinE) initiative, in which ECMWF is one of the partners.

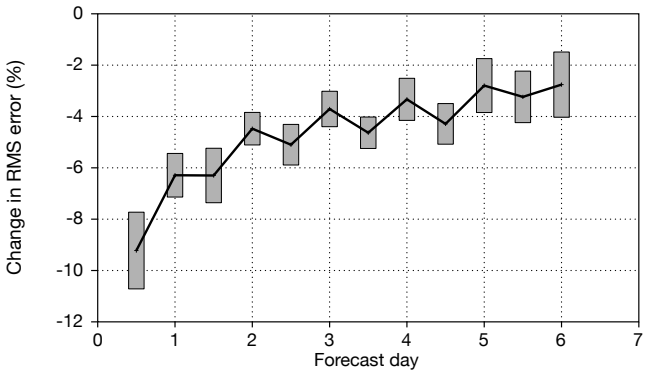

FIGURE 9 The impact of Cycle 49r1 on T2m forecasts verified against SYNOP observations (percentage change in root-mean-square error) for December 2021 to February 2022, 20°–90°N. The grey rectangles show 95% confidence intervals.

Further reading

Pauley, P. & **B. Ingleby**, 2022: Assimilation of in-situ observations. In: Park, S.K. & L. Xu (eds.) *Data Assimilation for Atmospheric, Oceanic and Hydrologic Applications*, Vol. IV, Springer.

de Rosnay, P., **P. Browne**, **E. de Boisséson**, **D. Fairbairn**, **Y. Hirahara**, **D. Schepers et al.**, 2022: Coupled data assimilation at ECMWF: current status, challenges and future developments, *Q. J. R. Meteorol. Soc.*, **148**(747), 2672–2702.

Boussetta, S., **G. Balsamo**, **G. Arduini**, **E. Dutra**, **J. McNorton**, **M. Choulga et al.**, 2021: ECLand: The ECMWF Land Surface Modelling System, *Atmosphere*, **12**, 723. *https://doi.org/10.3390/atmos12060723*

Arduini, G., **G. Balsamo**, **E. Dutra**, **J.J. Day**, **I. Sandu**, **S. Boussetta et al.**, 2019: Impact of a multi-layer snow scheme on near-surface weather forecasts, *Journal of Advances in Modeling Earth Systems*, **11**, 4687–4710. *https://doi.org/10.1029/2019MS001725*

Red sky at night... producing weather forecasts directly from observations

Tony McNally, Christian Lessig, Peter Lean, Matthew Chantry, Mihai Alexe, Simon Lang

ECMWF is embarking on a radical and ambitious project to investigate if weather forecasts can be made directly from meteorological observations, harnessing the power of machine learning (ML).

Highly skilful ML weather forecasts have challenged our approach to numerical weather prediction (NWP), prompting the development at ECMWF of our own ML forecasting system called AIFS (see the article on the AIFS in this Newsletter). Its performance is already highly competitive with that of established systems like Pangu-Weather and GraphCast. ML prediction systems (including the AIFS) have been trained to forecast future weather by learning from long historical records of past weather, typically provided by ECMWF reanalyses, such as ERA5. These datasets are well suited to training ML forecasts: they are highly accurate descriptions of the atmosphere and they provide conveniently gridded values of all required parameters, available at all locations and at all times for very long historical periods. In addition, our reanalysis datasets have been freely available to the wider research community, including the commercial sector. This has been a major factor in the rapid rise of ML forecast systems and the impressive levels of accuracy they have already achieved. However, while reanalyses, and initial conditions generated through data assimilation, are currently still crucial for ML forecasts, it is unclear if this will remain so in the future. Fundamentally, atmospheric analyses are just a fusion of an existing short-range forecast with the available meteorological observations, and an obvious question is if ML forecast systems could be trained and initialised directly from these observations. It is an intriguing science question, but also one that could potentially have huge implications for how weather forecasting is done in the future.

The use of observations in conventional forecast models

The many millions of meteorological observations made each day require highly sophisticated data assimilation (DA) systems to transform the raw measurements at irregular times and locations into data on a regular grid and into the variables required to initialise forecast models. This is an extremely challenging task because traditional forecast models demand initialisation on a fine spatial grid over the entire globe, even where there may be no observations, and with meteorological variables that may not be directly measured. For example, the overwhelming majority of observations come from weather satellites which measure thermal radiation emanating from broad vertical layers of the atmosphere. They do not directly measure temperature or humidity, and the extraction of this information requires a detailed understanding of complex radiative transfer processes in the atmosphere. Downward looking satellites cannot provide information on fine vertical scales, either. To meet the demands of forecast model initialisation, the measurements must be carefully blended with gridded fine-scale information from a previous short-range forecast background. ECMWF has been extremely successful in the development of its data assimilation system and has ambitious plans to extend its capability in a number of exciting directions. However, exploiting observations in this way remains a highly demanding scientific and technical activity.

Is there an alternative?

Much of the complexity described above stems from the fact that conventional forecast models demand initial conditions for all meteorological variables on a regular spatial grid. The strategy employed by conventional models to produce accurate weather forecasts is to represent the real atmosphere as comprehensively as possible, explicitly describing a myriad of fine-scale physical processes and interactions between variables at every grid point over the entire globe, from the surface up to the mesosphere. However, it has been demonstrated recently that ML systems operating with far fewer variables than conventional models and on significantly coarser spatial grids are capable of producing highly skilful medium-range forecasts of important weather parameters. This begs the intriguing question if ML forecast models could learn and be initialised directly from observations, obviating the need to convert observations to a fine grid of unmeasured physical variables dictated by the NWP model. If training of a ML model from observations was successful, large fractions of the conventional data assimilation process could be circumvented, potentially allowing forecasts to be produced more quickly as soon as observations

doi: 10.21957/tmc81jo4c7

are available. Direct Observation Prediction (DOP) with ML models may also be able to exploit additional observations that are currently not used by conventional data assimilation systems. For example, satellite radiance measurements in the visible part of the spectrum have such complex radiative transfer that they are not yet assimilated in global NWP systems. Yet in any animation of visible imagery one can clearly see the movement of weather patterns around the globe, and it seems entirely plausible that an ML forecast system could readily exploit this information to predict how weather patterns will evolve in the future. Another aspect is that an observation-based forecasting system does not require the approximative modelling of unresolved physical processes. These 'parametrizations' are a source of considerable uncertainties in conventional models. Instead, the ML model would rely on the feedback from small-scale processes that is captured in the observations to implicitly resolve processes that, for example, take place at small scales.

Preliminary investigations: observations predicting future observations

Research is at a very early stage, and the first question we are attempting to answer is how much predictive skill can be achieved when training on observations alone. When models like AIFS and GraphCast are trained from reanalysis datasets like ERA5, they are learning to predict the weather from past observations, but also from the conventional forecast model (the Integrated Forecasting System, IFS) used in the ERA5 data assimilation process. This conventional model plays an important role in the production of a coherent gridded representation of the atmospheric state. As a preliminary step, we are therefore investigating if an ML algorithm with only observations as input can be trained to predict future observations, completely removing any influence of a conventional forecast model in the training process. Our first experiments use microwave radiance measurements from satellites. These have the advantage that they provide high-quality observations with homogeneous coverage over

a **How does the prediction work?**

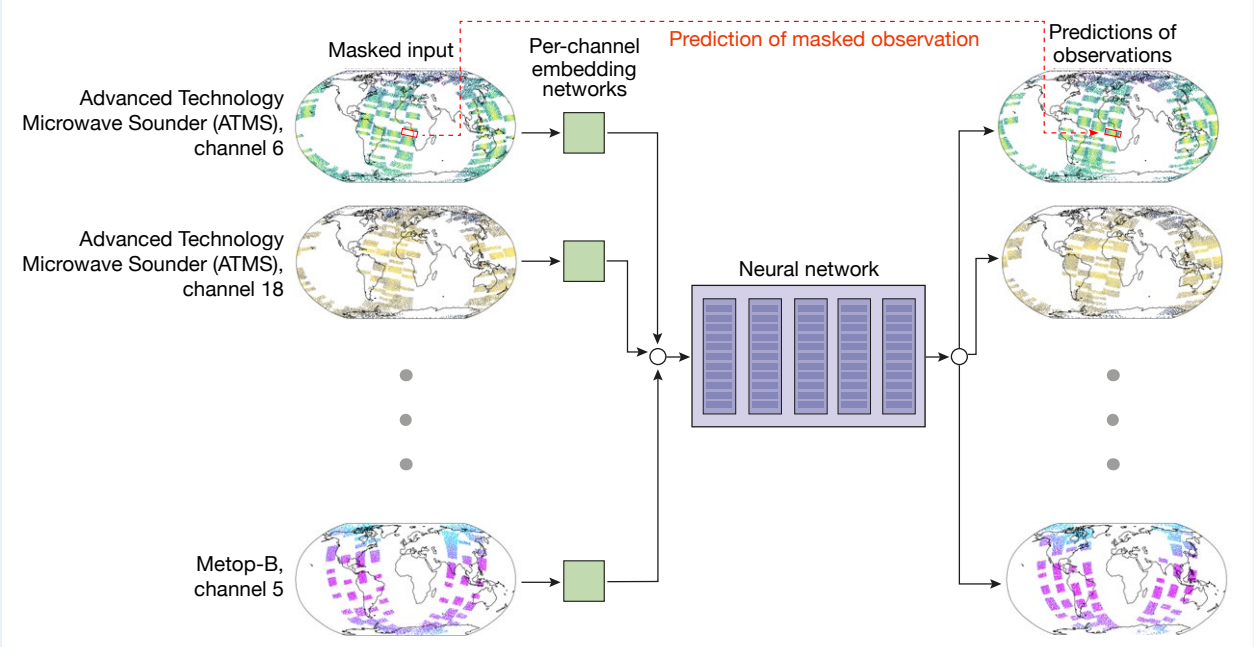

The network takes as input microwave radiance observations for several different channels, which are first subdivided into tokens, which represent all of the data in small location–time neighbourhoods. This huge amount of input training data (including the location-time information) is then mapped through a process called embedding to a highly compact and efficient vector representation for input to the transformer core (or backbone) neural network. Transformer networks are used extensively in many applications and are the driving force behind Large Language Models, such as ChatGPT. In here, the algorithm learns relationships between the observations at different spatial locations and times by randomly masking (or hiding) portions of the training data and creating predictions for the hidden values. The end result is that the network develops an ability to predict observations where they do not exist and, crucially, to predict observations at times when they do not exist – in other words, forecast future observations.

long historical periods of time. However, they also come with the limitation of rather coarse vertical and horizontal resolution. A prototype Transformer Neural Network (Box a) has been trained with ten years of real satellite observations to make 12-hour predictions, essentially using observations in one 12-hour assimilation time window as input and predicting the observations that would be obtained in the next 12-hour window. It can be seen in Figure 1 that the 12-hour predicted values are certainly realistic in terms of structure and variability compared to the real observations obtained 12 hours later. Furthermore, one can clearly see the movement of conspicuous meteorological features in the real observations from one 12-hour window to the next, and that the ML prediction correctly captures this movement.

These results are encouraging and suggest there is indeed predictive skill (at least over 12 hours) that can be learned from the observations alone. A next step is to challenge the algorithm with completely different types of observations. We will use land-surface temperature measurements from SYNOP weather stations, to test if meteorological variation can still be learned from the data in the presence of a strong diurnal cycle. This will also bridge the gap between the radiances used in the current experiments and variables of relevance to users, such as 2 m temperature or wind. Finally, in this preliminary part of the project we will investigate to what extent complementary information from different observing systems enhances the quality of the prediction. An exciting example of this will be combining visible and infrared imagery with SYNOP surface temperature observations. We know that in nature the presence of cloud cover can have a strong impact upon the magnitude of the land surface temperature diurnal cycle. Can the algorithm improve its prediction of surface temperature using cloud information learned from the imagery?

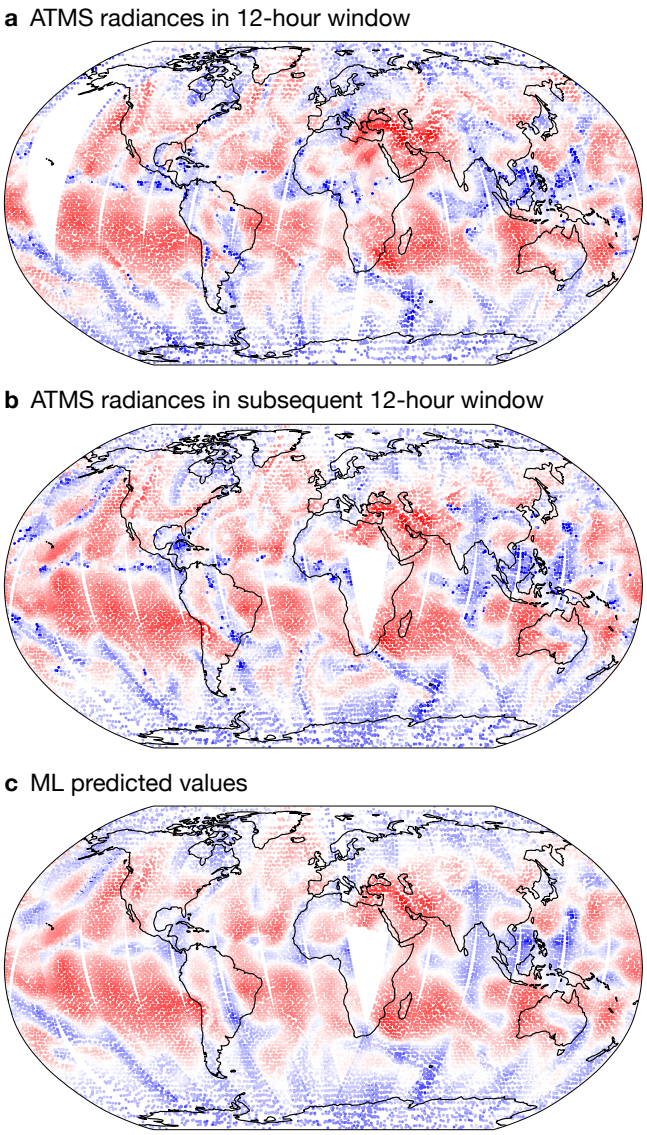

FIGURE 1 Here we show (a) observed Advanced Technology Microwave Sounder (ATMS) channel 18 radiances in an arbitrary 12-hour window provided as input to the ML prediction, (b) ATMS observations obtained in the subsequent 12-hour window, and (c) the ML predicted values.

How might we predict weather parameters directly from observations?

In the experiments described above, the ML algorithm is learning to predict future observations at real observation locations and times. However, provided there is sufficient information in the training data and with a suitable network architecture, ML algorithms are capable of learning spatial and temporal relationships between observations. Through this, they can generalise the predictions to locations and times where there are no direct measurements. Thus, if the algorithm can successfully learn to predict the surface temperature patterns from SYNOP stations, it should be possible to predict surface temperature at any location, even locations where there are no SYNOP stations. The same approach would apply for upper air information if the algorithm can learn to successfully predict radiosonde observations. All of this remains speculative at the moment. But with the existing network architecture and training protocol, we have identified a plausible mechanism allowing weather information for any time or location to be generated from a prediction algorithm trained directly on observations. There are, however, a number of different options for DOP that can be explored in the future (see Box b).

Moving towards longer-range predictions

The acid test of any observation-based prediction system is if it can be extended to forecast ranges of multiple days or even weeks. Data-driven forecast models (such as the AIFS, GraphCast and Pangu-Weather) trained from reanalysis data have clearly demonstrated this capability, so we have good reason

b Learning from observations: different approaches that could be taken

The current generation of analysis-driven ML models takes gridded (re)analysis data as input and is trained to predict the same fields at a future time (as shown under 1). Learning directly from observational data could take several different forms as illustrated in the figure. Firstly, observations could be used as a target 'truth' in the training, while still using gridded analysis data as input (shown under 2). For example, the existing AIFS could be trained to predict SYNOP observations – free from any systematic model biases present in the analysis datasets.

Alternatively, the ML model could be initialised directly from observational data (shown under 3–6). An ML model could be trained to map from input observations to the gridded 4D-Var analysis valid at the same time (shown under 3). By emulating 4D-Var in this way, a gridded analysis could be generated far more quickly than through the current computationally expensive data assimilation system.

However, any model biases present in the existing system would be inherited by the ML model, and such an approach would never be able to surpass the quality of the current 4D-Var analysis.

Panel 4 shows a scenario where the ML model takes observations as input but is trained to predict a gridded state in the future. This has the advantage that gridded forecasts could be generated for all model variables. However, a physical model and data assimilation would still be needed to generate the training dataset.

In the exploratory work discussed in this article, we are using a neural network which takes observations as input and is trained to predict the future state using observations as the ground truth (panel 5). This approach only includes observational data in the training dataset.

1 Predictions from analysis
e.g. current AIFS

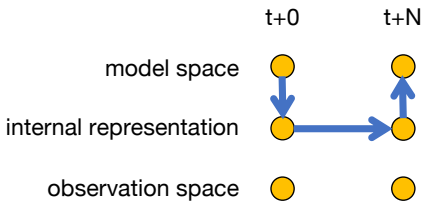

2 Predict observation targets from analysis input
e.g. fine tune AIFS to predict SYNOPS

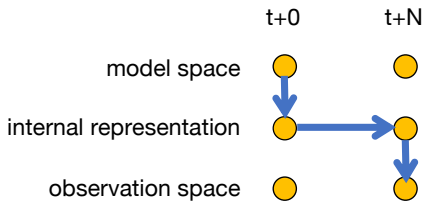

3 Learn the analysis
emulate 4D-Var

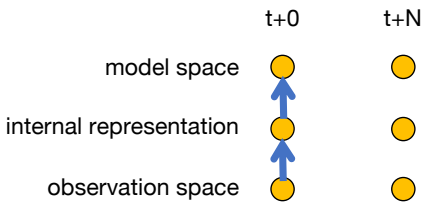

4 Predictions from observations
make predictions in model space, use reanalysis as truth

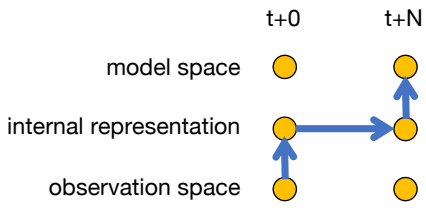

5 Predict future observations from observations
make predictions in observation space, use observations as truth

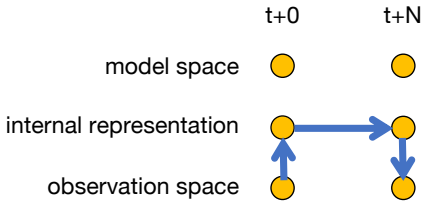

6 Other combinations

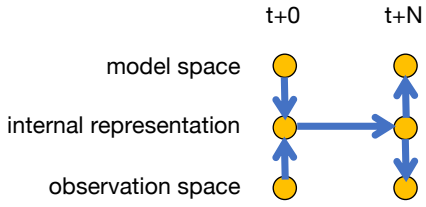

for optimism with DOP. To extend the range of predictions, we will investigate the use of the different types of neural network available (e.g. the Transformer Network described here, but we will also explore the Graph Networks employed by the AIFS). We will also explore different options for training longer-range predictions (auto-regressive vs fixed forecast length) to assess which is most suitable for longer-range direct observation forecasting. Here, our efforts will be accelerated by drawing extensively upon the experience gained in the development of the AIFS. Another interesting area of exploration will be enhancing the information content of the initialisation of the DOP algorithm with windows significantly longer than 12 hours (e.g. several days of observations). The aim will be to better inform on the past and current trajectory of weather systems and to provide an analogue of the background information used in conventional data assimilation. Here we will directly benefit from the highly sophisticated scientific and technical observation handling infrastructure that already exists at ECMWF.

Summary

We believe there is a strong strategic and scientific motivation for exploring this exciting new approach to weather forecasting. Direct observation-driven prediction is a very radical approach and, as such, pursuing this direction comes with no guarantee of success. However, we believe that our observation handling and assimilation experience, combined with our rapid uptake of ML technology, makes ECMWF very well placed to explore this pioneering and potentially paradigm-shifting area of research. This effort will very soon be complemented by a joint project with ECMWF Member States, where ML-assisted data assimilation will be addressed as one of the topics.

On-demand web plotting of observation monitoring statistics

Mohamed Dahoui, Cihan Sahin

Observation monitoring provides detailed statistical information on the quality and availability of the different components of the observing system monitored and used by ECMWF. The monitoring results are primarily produced to help improve the usage of observations within ECMWF's data assimilation system, which provides the initial conditions for forecasts. They are also used to provide feedback to observation data providers. Additionally, published observation monitoring statistics enable comparisons with results from other numerical weather prediction (NWP) centres and help identify the sources of differences between observations and the reference weather forecasting model. ECMWF makes a comprehensive set of observation monitoring statistics publicly available, covering almost all observations processed by ECMWF's data assimilation system (*https://www.ecmwf.int/en/forecasts/quality-our-forecasts/monitoring-observing-system*). This is also part of ECMWF's support for observation-related activities of the World Meteorological Organization (WMO). The monitoring website includes thousands of up-to-date products (time series, geographical maps, etc.), which are pre-plotted routinely (daily/weekly) and uploaded to the web. Unlike the regular access to forecast products, the access pattern to monitoring statistics is not regular and depends on each dataset and the interest of the user community. The objective of the work presented here is to replace the current framework with an on-demand system, enabling users to visualise statistics on the fly without the need to systematically pre-generate thousands of plots. Combined with an efficient caching system, the new framework will help optimise resources and will enable products to be refreshed more frequently. It will also offer more possibilities to access and inter-compare monitoring statistics.

Purpose of observation monitoring

Under the previous as well as the new arrangements, ECMWF makes available a wide range of statistical products on the quality, availability, usage status and estimated impact of satellite, in-situ and oceanic observations assimilated or monitored by ECMWF (see Table 1 at the end of this article). The statistical products are presented in various forms to highlight temporal evolution, vertical distribution, and geographical dependency. Although the monitoring products reflect ECMWF's usage of the data, the statistics are of benefit to the wider NWP community and data providers. It is, however, important to note that quantities based on departures from the background (a short-range forecast) and from the analysis (the best estimate of the current state of the Earth system) are affected by changes that are not necessarily related to the observations themselves. Such changes might be associated with variations in the accuracy of the reference forecasting model driven by atmospheric variability (short-lived signal), or with model or data assimilation upgrades (*https://www.ecmwf.int/en/forecasts/documentation-and-support/changes-ecmwf-model*). Therefore, a great deal of care is needed to interpret changes affecting long time series of departure statistics. Observation monitoring statistics are presented for selected data selection criteria to reflect the data characteristics and counts for different data sampling scenarios (All data, Used data, etc.). For a subset of observation types, statistics are computed and presented for different land–sea masks (sea, land, etc.) to highlight the sensitivity to the underlying surface.

Observation monitoring website

The observation monitoring website is organised by reference model (operational, the ERA5 reanalysis), data categories (satellite, conventional and oceanic), observation families (infrared radiances, all-sky radiances, atmospheric motion vectors, etc.), geophysical parameters (radiances, wind, temperature, bending angles, etc.), satellite sensors (Advanced Microwave Sounding Unit-A – AMSU-A; Microwave Humidity Sounder – MHS; Global Precipitation Measurement Microwave Imager (GMI), etc.); and data delivery streams (normal delivery; EUMETSAT Advanced Retransmission Service – EARS; etc.). Observation monitoring products were updated daily (time series, Hovmöller, scatter plots) and weekly (geographical maps of statistics). Most products covered the last two months.

Thousands of observation monitoring plots were routinely pre-generated and uploaded to the monitoring website regardless of how frequently these products were accessed. The procedure involved the processing of

doi: 10.21957/md3v5hk9ge

pre-computed gridded statistics, the generation of plots, and the transfer of products to the web infrastructure. The content of plots (layout, titles, colours, scales, etc.) was prescribed via plotting configuration files. This procedure was expensive and lacked flexibility.

New on-demand web plotting

The new on-demand framework (Figure 1) aims to make the access to monitoring statistics more efficient and flexible. It also provides more possibilities to explore the statistics. The underlying data are pre-processed every day using a set of gridded statistics computed by observation monitoring suites, which serve a range of operational and research requirements. The gridded statistics are converted to NetCDF format using a template compatible with the ECMWF web infrastructure. The conversion is controlled by a single configuration file per data type. This file defines the temporal resolution of statistics, the geographical areas of interest, the length of time series, the data selection to be considered, land–sea masks to be included, observation quantities to be added, and the overlay of statistics from different satellites. The conversion configuration files are, however, bound by the content of pre-computed gridded statistics. Converted NetCDF files are then pushed to web machines, where the data are indexed and integrated in a data store ready to be used by the on-demand plotting system. Housekeeping tools were integrated to control the retention period of statistics. The web plotting engine has been developed and integrated in the web front end. It is mainly based on the JSON user interface enabling users to make a plotting selection (data type, area, data selection, period, etc). The selection is then used to interrogate the NetCDF files and return the data to be plotted by executables based on ECMWF's meteorological plotting software Magics (*https://confluence.ecmwf.int/display/MAGP/Magics*). The JSON user interface controls all aspects of the on-demand plotting. This includes:

- The structure and hierarchy of observation monitoring statistics
- The name of underlying NetCDF files to be used for each dataset
- The content of the plots: number and content of panels for time series; observation quantities to be included for geographical maps and Hovmöller diagrams; areas, data streams, flags, etc.
- Titles, scales, colours, fonts – default settings are used if nothing is specified
- Settings to overlay statistics from different sources
- Available lengths of time series
- Retention period for daily updates.

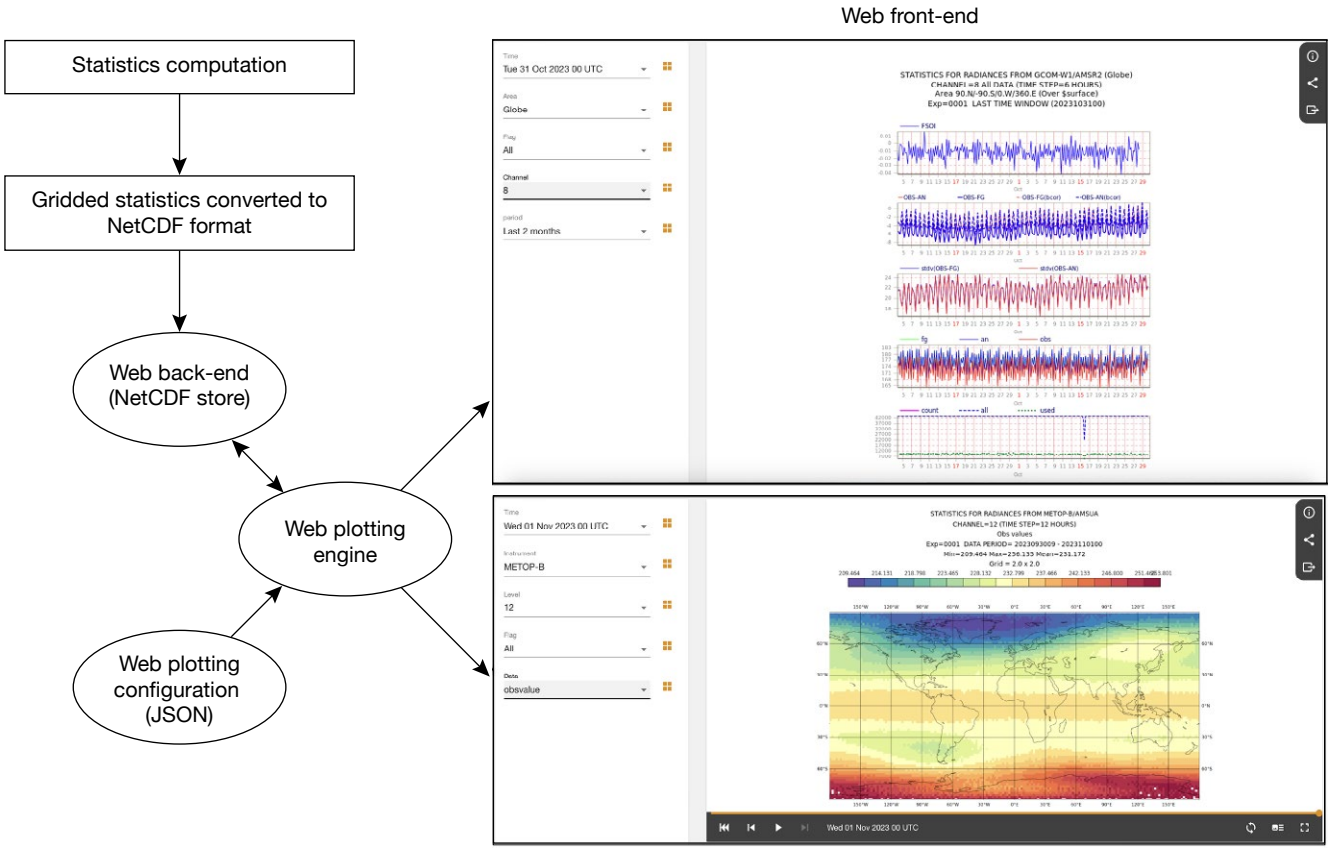

FIGURE 1 Diagram of the on-demand web plotting framework of observation monitoring statistics.

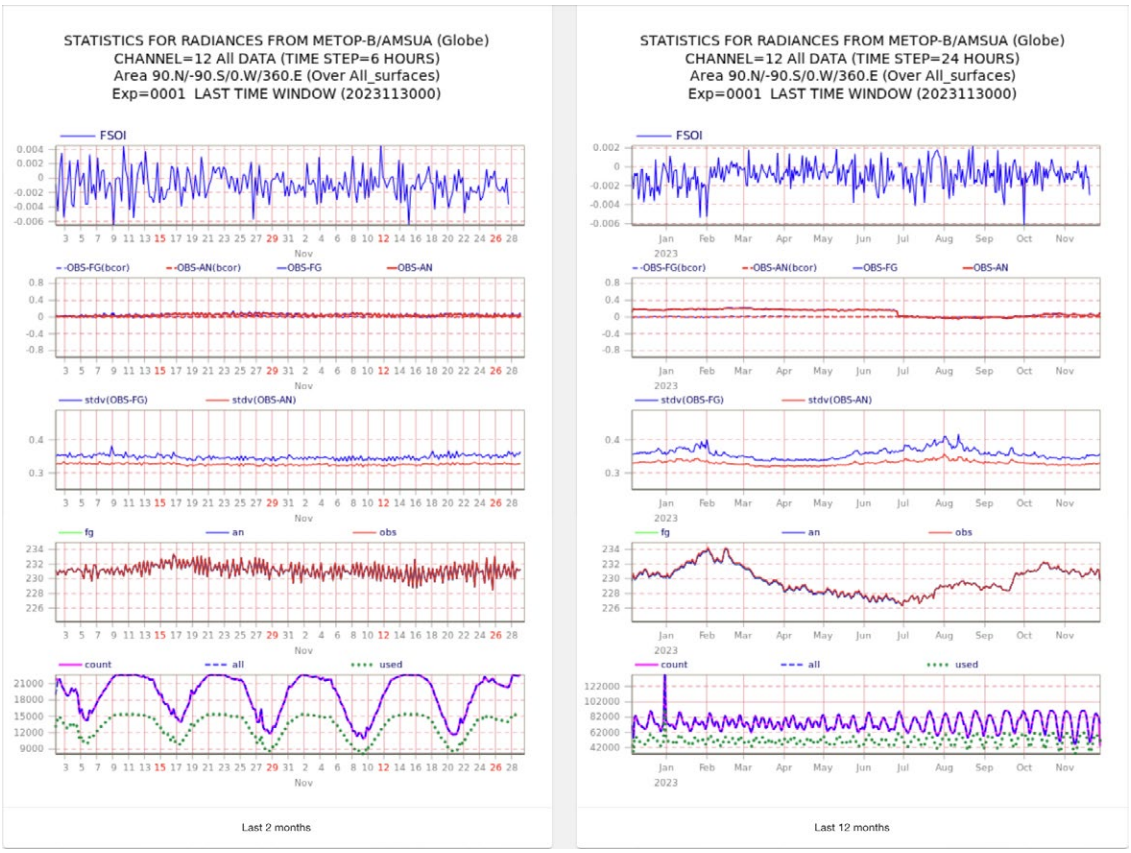

FIGURE 2 Overview of time series of statistics from the AMSU-A instrument, Channel 12, on the Metop-B satellite for two time lengths (two months and 12 months), as shown on the new web plotting facility.

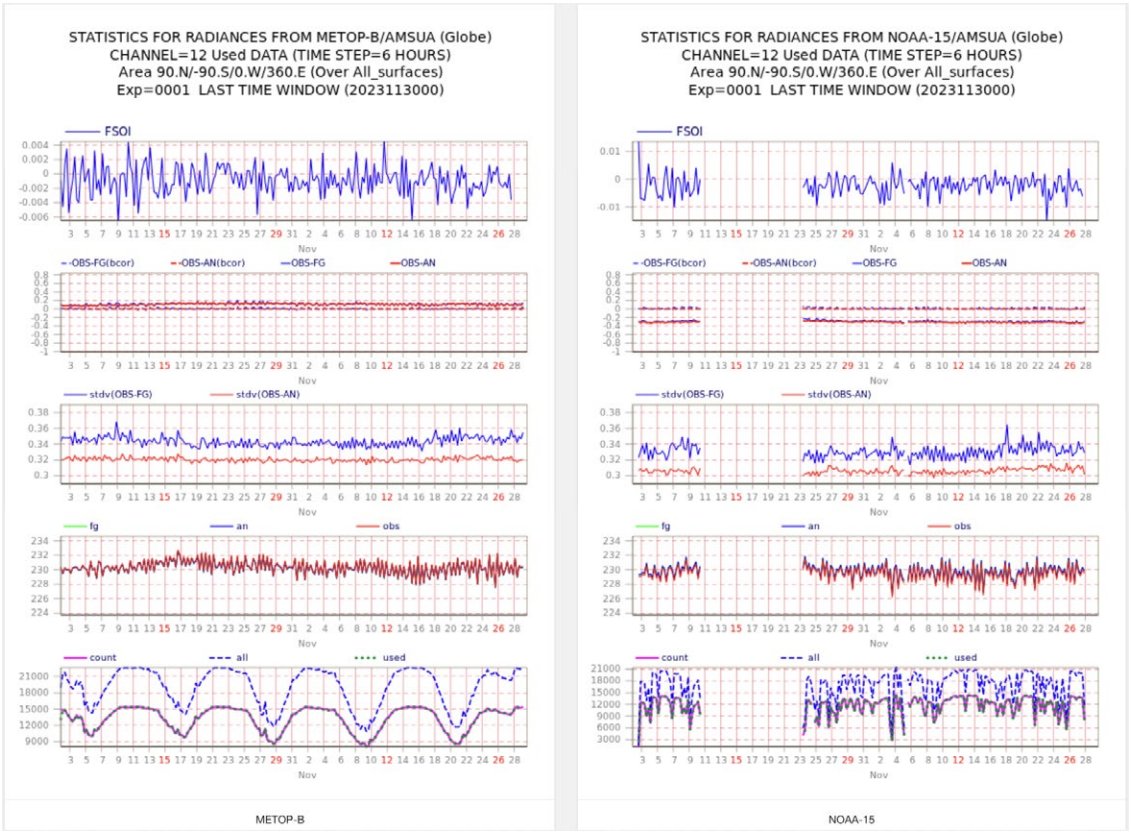

FIGURE 3 Overview of time series of statistics from the AMSU-A instrument, Channel 12, from two satellites, as shown on the new web plotting facility.

Observation category	Geophysical parameter	Instrument	Satellites	Statistical products
Satellite observations	Infrared radiances	IASI	Metop-B, Metop-C	Time series, Hovmöller, geographical maps, Jacobians
		AIRS	AQUA	
		CrIS	S-NPP, NOAA-20, NOAA-21	
		HIRS	NOAA-19	Time series, Hovmöller, geographical maps, Jacobians
	Microwave radiances	AMSU-A	Metop-B, Metop-C, NOAA-15, NOAA-18, NOAA-19	Time series, Hovmöller, geographical maps, Ascending/descending stats (some instruments), Jacobians
		MHS	Metop-B, Metop-C, NOAA-15, NOAA-18, NOAA-19	
		ATMS	S-NPP, NOAA-20, NOAA-21	
		AMSR2	GCOM-W1	
		SSMIS	DMSP-17, DMSP-18	
		GMI	GPM	
		MWHS2	FY-3C,FY-3D, FY-3E	
		MWRI	FY-3D	
	Geostationary radiances	ABI	GOES-16, GOES-18	Time series, Hovmöller, geographical maps
		SEVERI	MET-9, MET-10	
		AHI	HIMAWARI-9	
	Atmospheric Motion Vectors	SEVERI	MET-9, MET-10	Time series, Hovmöller (latitudes versus time, vertical layers versus latitudes), geographical maps
		ABI	GOES-16, GOES-18	
		AHI	HIMAWARI-9	
		AVHRR	NOAA-15, NOAA-18, NOAA-19, METOP-B, METOP-C, Dual-Metop	
		MODIS	AQUA, TERRA	
		INSAT	INSAT-3D	
		VIIRS	S-NPP, NOAA-20	
		VISSR	FY-2G	
		LEO-GEO		
	GNSS Radio occultation	GNSS-RO	Metop-B, Metop-C, COSMIC-2E (6 satellites), TERRA-SAR-X, KOMPSAT-5, PAZ, Sentinel-6, PlanetIQ, SPIRE, GRACE-D,	Time series, Hovmöller (vertical layers versus time), geographical maps, vertical profiles
	Surface winds	ASCAT	Metop-B, Metop-C	Time series, Hovmöller, geographical maps
		HSCAT	HY-2C, HY-2D	
		Altika	SARAL	
	Wave height	Altika	SARAL	
	Snow cover	IMS	IMS	
	Soil moisture	ASCAT	Metop-B, Metop-C	Time series, Hovmöller, geographical maps, scatter plots
Conventional observations	Surface pressure	SYNOP, Metar, Drifter buoys, Moored buoys, Ship		Time series, geographical maps
	Upper-air Temperature	Radiosondes, Amdar, ADS-C, Airep		
	Upper-air wind	Radiosondes, Amdar, ADS-C, Airep, Pilot, Mode-S		
	Upper-air humidity	Radiosondes, Amdar		
	2 m temperature	SYNOP, Metar		
	2 m humidity	SYNOP		
	Snow depth	SYNOP		
	Surface wind speed	Ship, Drifter buoys, Moored buoys		
Ocean observations	Potential temperature	ARGO, Moored buoys, Mammals, CTDs, XBTs		Time series, Hovmöller (depth versus time), geographical maps, vertical profiles, histograms
	Salinity	ARGO, Moored buoys, Mammals, CTDs, XBTs		

TABLE 1 List of available statistics on the observations monitoring website.

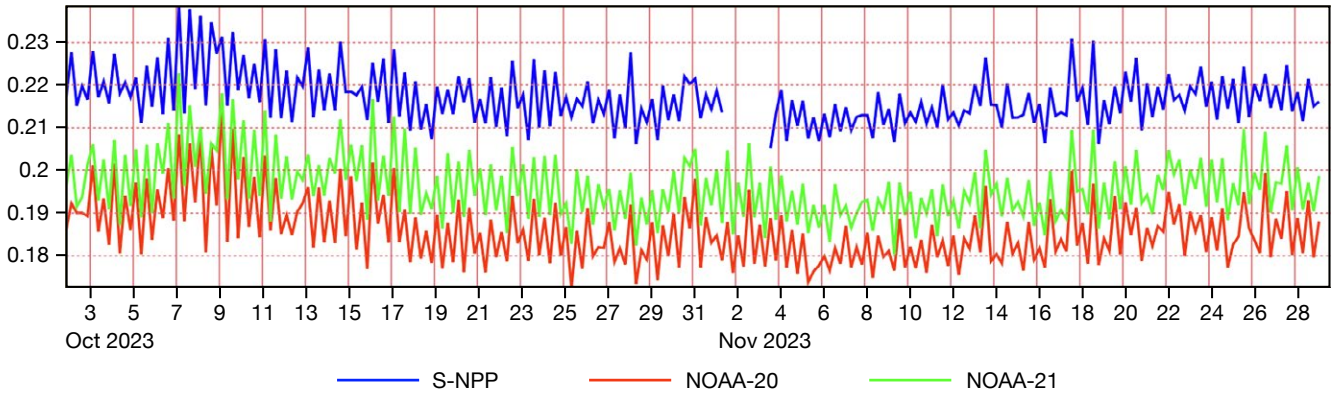

FIGURE 4 Overview of time series showing the standard deviation of observation minus first guess (short-range) forecast statistics from the Advanced Technology Microwave Sounder (ATMS), Channel 12, from three available satellites: the US Suomi National Polar-orbiting Partnership satellite (S-NPP), and two of the US National Oceanic and Atmospheric Administration satellites (NOAA-20 and NOAA-21).

Figures 2 and 3 show various time series obtained using the new system.

Being integrated in ECMWF's OpenCharts web framework, the user interface enables users to compare statistics for each data selection axis (available satellites, areas, channels, data selection, etc.). This facility can be of great interest. The Json files can be easily updated and pushed to the web interface, enabling immediate update of the layout without any need to touch the underlying data. The new framework benefits from a powerful cache system that enables fast access to plots frequently used. The performance remains good to access all products.

The on-demand plotting of observation monitoring makes it possible to perform daily updates of all products (instead of weekly), enables plotting of time series at various temporal lengths (two months, 12 months, and the whole lifetime of the data), and makes it possible to overlay statistics from available satellites in one and the same plot (Figure 4).

Migration timeline

With thousands of products to migrate, it was decided to follow a stepwise approach to migrate individual data types to the new system. This fits well with the OpenCharts framework, in which the user interface is fed from static plots or on-demand plotting. Infrared radiances, microwave radiances and geostationary radiances were the first to be migrated to the new framework. The process was complete by the end of 2023.

Conclusion and perspectives

The migration to on-demand web plotting of observation monitoring is now complete. The new framework leads to efficient access to up-to-date observation statistics and offers additional possibilities to compare statistics and access long-term time series. The direct interaction between web client and NetCDF files will enable more capabilities in the future, such as zooming, overlay with external fields, access to grid point values, and access to time series over custom areas defined by users.

ECMWF Council and its committees

The following provides some information about the responsibilities of the ECMWF Council and its committees. More details can be found at:

http://www.ecmwf.int/en/about/who-we-are/governance

Council

The Council adopts measures to implement the ECMWF Convention; the responsibilities include admission of new members, authorising the Director-General to negotiate and conclude co-operation agreements, and adopting the annual budget, the scale of financial contributions of the Member States, the Financial Regulations and the Staff Regulations, the long-term strategy and the programme of activities of the Centre.

President Prof. Penny Endersby *(UK)*

Vice President Dr Roar Skålin *(Norway)*

Policy Advisory Committee (PAC)

The PAC provides the Council with opinions and recommendations on any matters concerning ECMWF policy submitted to it by the Council, especially those arising out of the four-year programme of activities and the long-term strategy.

Chair Ms Virginie Schwarz *(France)*

Vice Chair Prof. Dr Maarten van Aalst *(Netherlands)*

Finance Committee (FC)

The FC provides the Council with opinions and recommendations on all administrative and financial matters submitted to the Council and exercises the financial powers delegated to it by the Council.

Chair Mr Lukas Schumacher *(Switzerland)*

Vice Chair Ricardo José Squella de la Torre (*Spain*)

Scientific Advisory Committee (SAC)

The SAC provides the Council with opinions and recommendations on the draft programme of activities of the Centre drawn up by the Director-General and on any other matters submitted to it by the Council.
The 12 members of the SAC are appointed in their personal capacity and are selected from among the scientists of the Member States.

Chair Prof. Dr Thomas Jung *(Germany)*

Vice Chair Dr Susanna Corti *(Italy)*

Technical Advisory Committee (TAC)

The TAC provides the Council with advice on the technical and operational aspects of the Centre including the communications network, computer system, operational activities directly affecting Member States, and technical aspects of the four-year programme of activities.

Chair Dr Sarah O'Reilly *(Ireland)*

Vice Chair Ms Anne-Cecilie Riiser *(Norway)*

Advisory Committee for Data Policy (ACDP)

The ACDP provides the Council with opinions and recommendations on matters concerning ECMWF Data Policy and its implementation.

Chair Ms Monika Köhler *(Austria)*

Vice Chair Anne Kristensen *(Norway)*

Advisory Committee of Co-operating States (ACCS)

The ACCS provides the Council with opinions and recommendations on the programme of activities of the Centre, and on any matter submitted to it by the Council.

Chair Mr Abdelfetah Sahibi *(Morocco)*

ECMWF publications

(see *www.ecmwf.int/en/research/publications*)

Technical Memoranda

914 **Quintino**, **T.**, **I. Russell**, **D. Tipping** & **D. Figala**: Impact of using Github enterprise for open development. *November 2023*

913 **Massart**, **S.**: Extended control variable (XCV): skin temperature background correction for the assimilation of clear-sky microwave radiances. *October 2023*

912 **Bormann**, **N.**, **L. Magnusson**, **D. Duncan** & **M. Dahoui**: Characterisation and correction of orbital biases in AMSU-A and ATMS observations in the ECMWF system. *October 2023*

EUMETSAT/ECMWF Fellowship Programme Research Reports

62 **Steele**, **L.**, **N. Bormann** & **D. Duncan**: Assimilating FY-3E MWHS-2 obs, and assessing all-sky humidity sounder thinning scales. *December 2023*

ECMWF Calendar 2024

Feb 5–8	Online training course: Use and Interpretation of ECMWF products
Mar 4–8	Training course: Data assimilation
Mar 11–15	Training course: EUMETSAT/ECMWF NWP-SAF satellite data assimilation
Mar 18–22	Training course: Machine learning for weather prediction
Apr 8–12	Data policy meetings of ECMWF, EUMETSAT & EUMETNET
Apr 10–12	5th Workshop on Waves and Wave-Coupled Processes
Apr 23	Policy Advisory Committee (virtual)
Apr 24	Finance Committee (virtual)
May 7–10	ECMWF–ESA Machine Learning Workshop (Italy)
May 13–17	OpenIFS User Meeting, Reading
Jun 10–13	8th CAMS General Assembly
Jun 11–13	ROM SAF workshop
Jun 17–20	7th C3S General Assembly
Jun 19–20	Council (Brussels)
Sep 9–12	Workshop on Diagnostics for Global Weather Prediction
Sep 30–Oct 3	Training course: Use and interpretation of ECMWF products
Oct 7–9	Scientific Advisory Committee
Oct 10–11	Technical Advisory Committee
Oct 21–22	Finance Committee
Oct 22	Policy Advisory Committee
Nov 11–15	Training course: Numerical methods for weather prediction
Dec 10–11	Council

Contact information

ECMWF, Shinfield Park, Reading, RG2 9AX, UK

Telephone National 0118 949 9000

Telephone International +44 118 949 9000

ECMWF's public website *www.ecmwf.int/*

E-mail: The e-mail address of an individual at the Centre is firstinitial.lastname@ecmwf.int. For double-barrelled names use a hyphen (e.g. j-n.name-name@ecmwf.int).

For any query, issue or feedback, please contact ECMWF's Service Desk at *servicedesk@ecmwf.int*. Please specify whether your query is related to forecast products, computing and archiving services, the installation of a software package, access to ECMWF data, or any other issue. The more precise you are, the more quickly we will be able to deal with your query.

ECMWF

Newsletter | **No. 178** | Winter 2023/24

European Centre for Medium-Range Weather Forecasts

www.ecmwf.int